INVESTIGATING THE LINK BETWEEN TROPOSPHERIC BLOCKING AND SUDDEN STRATOSPHERIC WARMING IN THE NORTHERN HEMISPHERE

A Dissertation

Presented to the Faculty of the Graduate School

of Cornell University

in Partial Fulfillment of the Requirements for the Degree of

Doctor of Philosophy

by

Michael Ewens Kelleher

January 2014

INVESTIGATING THE LINK BETWEEN TROPOSPHERIC BLOCKING AND SUDDEN STRATOSPHERIC WARMING IN THE NORTHERN HEMISPHERE

Michael Ewens Kelleher, Ph.D.

Cornell University 2014

The link between sudden stratospheric warmings (SSWs) and tropospheric blocking events has been heavily investigated, both in the composite sense, as well as individual case studies. The implications of improved SSW forecasting include improved surface weather predictability, as the warmings have long time scale impacts on the troposphere.

In this study, the National Center for Environmental Prediction/National Center for Atmospheric Research (NCEP/NCAR) Reanalysis (Kalnay et al., 1996), and NASA's Modern Era Retrospective Reanalysis (MERRA) (Rienecker et al., 2011) data sets were used to differentiate blocking events that occur without the presence of any stratospheric warming from those that are linked with warmings, either preceding or following it. This was accomplished through the generation of composites of geopotential height fields, Ertel's potential vorticity on the longitude-time plane and averaged over the polar cap, zonal mean zonal wind diagnosis, and meridional eddy heat flux.

It was found that indeed there are several distinguishing features that discriminate blocking events associated with SSWs from those that are not. Firstly, the zonal mean zonal wind appears to link the stratosphere with the troposphere during blocking events associated with SSWs, while no such link appears in the

events that are not. The meridional eddy heat flux features large ten-day averaged values in the period before and just after block onset in the SSW associated composites, while it is absent in the non-associated composites. The polar cap PV average also separates the SSW associated events from the non-events, with an anticyclonic anomaly before block onset, and cyclonic anomaly after onset, whereas the non-events feature only a minimal change in tropospheric PV.

The tropospheric polar cap PV and meridional eddy heat flux were used as forecast indicators for historical SSW events in both data sets, and presented nominal skill over climatology. A statistical comparison was also performed on the duration of blocking, that indicates that longer duration blocks are more likely associated with SSW events, but this was only statistically significant in the NCEP/NCAR Reanalysis, and was not replicated with the MERRA data set.

BIOGRAPHICAL SKETCH

Michael Ewens Kelleher was born near the shore of Lake Ontario in Oswego, New York to William and Carolyn Kelleher. He attended school in the Oswego City School district and graduated from Oswego High School. During his school career, he was an active member of the Boy Scouts of America, ultimately achieving the rank of Eagle Scout. Upon graduation from high school, he attended SUNY Oswego, earning undergraduate degrees in in Meteorology and Applied Mathematics. While at SUNY Oswego, he participated in the Oswego State Student Chapter of the AMS. This included becoming Treasurer and Vice President as well as serving on the committee of the first and second annual Lake Effect Conference (now called Great Lakes Atmospheric Science Symposium). Michael is also a student member of the American Meteorological Society (AMS) and Sigma Xi, the Scientific Research Society. In his senior year at SUNY Oswego, he had the opportunity to do research with Dr. Steven Skubis on large scale and wave dynamics. It was this research that ultimately led him to Cornell University to work with Dr. Stephen Colucci, where he earned his Master of Science degree in 2010, researching the stratospheric impact on a particular blocking event. He has continued on at Cornell working with Dr. Colucci on this more expanded study of blocking and the stratosphere.

For my fiancée Andrea, your friendship and support mean the world to me!

For my family, Dad, Mom and Sally, your support and encouragement made this possible!

ACKNOWLEDGEMENTS

I would like to acknowledge the invaluable guidance of my adviser Dr. Stephen Colucci, who helped guide me through the daunting research tasks before me. I would also like to acknowledge the assistance and support of my minor advisers Drs. Gang Chen, Peter Diamessis and Natalie Mahowald.

I would also like to acknowledge the support of my fellow graduate students Steve Jessup, Christina Patricola, Rachel Scanza, Marcus Walter, Huang "Caesar" Yang, Wenxiu "Tracy" Sun, Yun Zheng, Alex Burrows, and Drew Montreuil for their friendship and for help along the way. Also, Brian Belcher and Marty Sullivan for providing technical assistance. In addition, I would like to acknowledge Pam Vitale for her incalculable assistance.

The schematic diagrams were created in Inkscape, and the figures were created using the NCAR Command Language (NCL). The NCEP/NCAR Re-analysis was provided by the Earth System Research Laboratory, Physical Sciences Division available at http://www.esrl.noaa.gov/psd/data/reanalysis/reanalysis.shtml. NASA's MERRA data was provided by NASA's Global Modeling and Assimilation Office and is available at http://gmao.gsfc.nasa.gov/merra/.

This research was funded in part by a grant from the National Science Foundation.

TABLE OF CONTENTS

LIST OF TABLES

LIST OF FIGURES

CHAPTER 1

INTRODUCTION

Tropospheric blocking is defined by its longevity and large spatial extent, and has been of interest to the atmospheric science community since at least the late 1940s (Rossby (1945), Namias (1947), Rex (1950)). A blocking event can interrupt the typical zonal (west-to-east) flow in the mid-latitudes for several days or more, and can result in temperature (Carrera et al., 2004) and precipitation (Trenberth and Guillemot, 1996) extremes, an idealized blocking event pattern can be seen in figure 1.1. In addition, a feedback mechanism between snow cover and blocking has been found (García-Herrera and Barriopedro, 2006), whereby local snow cover influences blocking frequency, which in turn influences snow cover on a larger scale. Blocking has also been linked with stratospheric variability by several studies, including Quiroz (1986), Martius et al. (2009), Garfinkel et al. (2010), Nishii et al. (2011) among others.

The wintertime stratosphere is defined by the polar stratospheric vortex, a strong cyclonic circulation that spins up each fall, and decays each spring, whose climatological average is depicted in figure 1.2. Approximately 8 times per decade (based on 50 observed events in 62 years), the vortex will undergo a major sudden warming where the vortex is displaced off the pole, or is split into two smaller vortices (Charlton and Polvani, 2007). In addition, minor warmings occur around 9 times per decade (56 events in 62 years), where the vortex or vortices only slightly displaces away from the pole. In this paper, a stratospheric sudden warming

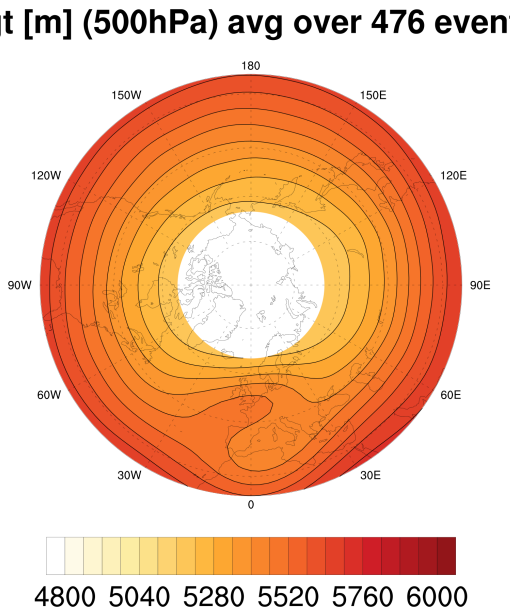

Figure 1.1: Average geopotential height [m] 500 hPa for all blocking events detected in NCEP/NCAR reanalysis using methods defined in section 2.2. Shows the average dipole blocking signature centered at 0°W, 45°N.

(SSW) will be referred to as a major SSW or minor SSW depending on definitions given in section 2. Stratospheric variability has been shown in the past to be an important influence on tropospheric weather systems (Baldwin and Dunkerton, 2001), thus its importance in enhancing predictability (Thompson et al., 2002), (Baldwin et al., 2003). The Aleutian High, a high pressure system over the Aleutian archipelago, can also be prominent during sudden warmings, which Harvey and Hitchman (1996) found to be related to subsidence and tropical to extratropical wintertime transport.

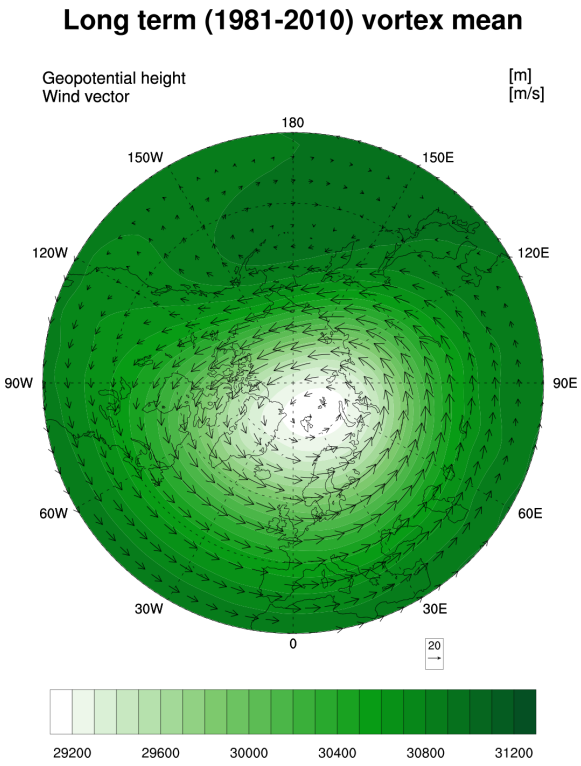

Figure 1.2: Height (shaded) and wind (vectors) at 10 hPa for November–March long term (1981-2010) mean using NCEP reanalysis. Polar stratospheric vortex shown centered at approximately 85°N, 45°E.

It is well established that tropospheric disturbances must be of sufficiently large scale, with a westerly or weak easterly stratospheric vortex for the transport of energy to the stratosphere (e.g. Charney and Drazin (1961), Scinocca and Haynes (1998)). Sudden stratospheric warmings have been heavily studied including Charlton and Polvani (2007), who employed an observational approach to compare the dynamics of split and displaced vortex major warming events, using 45 years of data and finding 28 or 29 events depending on data-set used, Matthewman and Esler (2011), who used an ideal mathematical model to examine

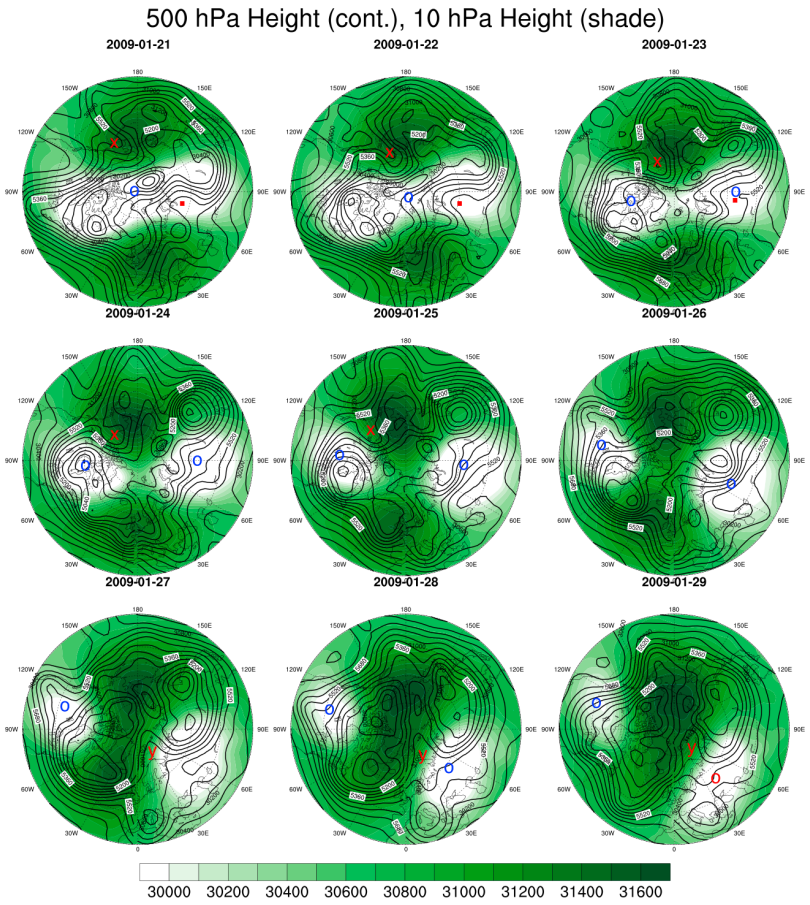

Figure 1.3: Geopotential height at 10 hPa (shaded) and 500 hPa (contoured) in meters for 21-29 January 2009 using NCEP reanalysis. SSW event key date is 25 January 2009. Red "x" indicates a blocking event before SSW with the red dot indicating a concurrent large scale ridge, red "y" indicates a blocking event following the warming. Blue "o" indicates approximate center(s) of polar stratospheric vortex. Note that splitting occurs before SSW key date.

split vortex warmings, finding that these can occur without a tropospheric planetary wave source and Esler and Matthewman (2011) using the same approach for displacement warmings, and finding that external wavenumber 1 resonant forcing is needed.

Minor stratospheric sudden warmings, while less prominent, are also represented in the current literature. Mitchell et al. (2010) found that minor warming events can affect the geometry of the polar vortex more than major warmings, and used this information to develop a detection method based on moments (Mitchell et al., 2012), (Seviour et al., 2013). Koermer et al. (1983) found that the strength of the polar night jet was the determining factor in differentiating major and minor warmings in a numerical model.

The variability in the stratosphere has been found to be strongly related to the vertical component of Eliassen-Palm flux by Christiansen (2001); this is supported by Sjoberg and Birner (2012), who found that the duration of meridional eddy heat flux (proportional to the vertical component of E-P flux) was important in major and minor SSW events. They also found that the magnitude of the heat flux was not as important, but in the composite of all SSW events, it was larger than climatology, though not greater than one standard deviation.

As mentioned above, Martius et al. (2009) related tropospheric blocking to stratospheric variability. They found that the wavenumber 1 (displacement) events and the wavenumber 2 (split) events are preceded by blocking events in different regions. Wave 1 events tend to be preceded by blocking in the Atlantic basin, whereas wave 2 events are preceded by blocking in the Pacific basin, or simultaneous blocking in both basins. An example of a wavenumber 2 SSW event, associated with Pacific blocking can be seen in figure 1.3. Martius et al. (2009) differentiates different types of SSW events from one another and though it does not differentiate the blocking events themselves, supports the idea that the location of blocking is important. A similar result comes from Garfinkel et al. (2010), where it was found that tropospheric anomalies of E-P flux and geopotential height are strongly correlated with polar vortex weakening when in phase with climatological planetary scale waves. This result was found in both reanalysis data as well as the Whole Atmosphere Community Climate Model (WACCM), though it was weaker in WACCM.

Similarly, Nishii et al. (2011) found that the location of blocking was important to vortex breakdown. They also found that blocking events which are nearly stationary are more likely to cause stratospheric warming, whereas blocking events that move toward climatological planetary scale troughs are likely to cause stratospheric cooling. They also state an important point, that blocking events are far more frequent than sudden warmings, thus it is important to be able to distinguish blocking events that are associated with SSWs from those that are not. They

suggest that studies like Taguchi (2008) do not find a statistical link due to the inclusion of events in which the stratosphere is cooled.

The focus of this study has been on the differentiation of blocking events that are associated with sudden stratospheric warmings from those that are not through several questions stated here. Is there a statistical relationship between block duration or location and SSW proximity? Do these blocking events evolve differently in the height or PV fields? As it has been previously found during SSW events, is the Aleutian High present during blocking events not associated with warmings? The duration meridional eddy heat flux has been found to be linked to SSW events, can this differentiate between blocking events associated or not associated with SSW events? If there are differences what spatial or temporal scales are there differences? Does the polar-cap PV differ? Do blocking events associated with minor warmings exhibit similar differences? Can any of the quantities used to distinguish events be used to predict SSW events?

CHAPTER 2

METHODS AND DATA

2.1 Data

2.1.1 NCEP

The National Center for Environmental Prediction/National Center for Atmospheric Research (NCEP/NCAR) re-analysis (Kalnay et al., 1996) was used in this research as the first data set for analysis. It spans 1948-2012, and has a horizontal resolution of 2.5°x 2.5°, and interpolated to 17 pressure levels (1000hPa-10hPa).

The NCEP-NCAR reanalysis has been found to be a relatively good representation of real atmosphere conditions in some areas, including profiles of wind and temperature over the Tibetan plateau (Bao and Zhang, 2012), with errors on the order of ± 2 m/s or K respectively. Though there are some issues with the data, especially its representation of near-surface weather (e.g. Anderson and Arritt (2001) and Smith et al. (2001)), and the stratosphere (Trenberth and Stepaniak, 2002).

2.1.2 MERRA

NASA's Modern-Era Retrospective Re-Analysis (Rienecker et al., 2011) was also used to expand the results, and to gain improvements in the representation of the stratosphere and resolution, both vertical and horizontal. The horizontal resolution of the assimilated data is 1.25°x 1.25°interpolated to 42 pressure levels spanning 1000 - 0.1 hPa. This is generated from a large set of observational data (detailed in appendix B of Rienecker et al. (2011)) including satellite (EOS, Terra and MODIS) winds, surface land, ship, and buoy observations, radiosonde and dropsonde soundings and satellite radiance data.

Brunke et al. (2011) found that MERRA was slightly biased in ocean surface turbulence fluxes compared to observational data, though its biases were lower than that of other reanalyses including the NCEP/NCAR reanalysis. Bosilovich et al. (2011) found that MERRA performed well with respect to global mean precipitation and energy budgets, but is relatively weak over ocean basins in both quantities. The authors of Rienecker et al. (2011) also note that stratospheric performance was tested, and both the quasi-biennial oscillation (QBO) and semiannual oscillations (SAO) in the tropics were realistically represented in MERRA's stratosphere.

2.2 Block detection

To detect blocking events, a wave breaking index based on Pelly and Hoskins (2003), which used potential temperature on potential vorticity surfaces, was adapted for use with Ertel's potential vorticity (EPV) on isobaric surfaces. This is detailed in equation 2.1, where ϕ is latitude, λ is longitude, (ϕ_0, λ_0) is the initial point, $\phi_{-1} = \phi_0 - \Delta\phi/2$ and $\phi_{+1} = \phi_0 + \Delta\phi/2$, $\lambda{-}1 = \lambda_0 - \Delta\lambda$ and $\lambda{+}1 = \lambda_0 + \Delta\lambda$. A_S and A_N are the areas over which each average is taken.

$$B(t, \phi_0, \lambda_0) = \left(\int_{\lambda_{-1}}^{\lambda_{+1}} \int_{\phi_{-1}}^{\phi_0} Q d\phi d\lambda \right) / A_S - \left(\int_{\lambda_{-1}}^{\lambda_{+1}} \int_{\phi_0}^{\phi_{+1}} Q d\phi d\lambda \right) / A_N \tag{2.1}$$

Results consistent with traditional blocking definitions were given when $\Delta\phi$ was set as 15°, and $\Delta\lambda$ was set as 5°. The schematic illustrated by figure 2.1

Thus, where the blocking index (B) is positive, there is a reversal of the climatalogical north-south gradient of PV, and therefore wave breaking. For a blocking event to be identified, there must be a significant wave breaking event within 30°(15°north or south) of the mid-latitude climatalogical jet. A significant event in this case means that 96% of points within a 20°longitude, 15°latitude box are positive for at least 3 days. The pressure level used here was 250 hPa, though the results are not very sensitive to changes in pressure level; the same parameters were used at 500 and 200 hPa with only slight variations in frequency of events.

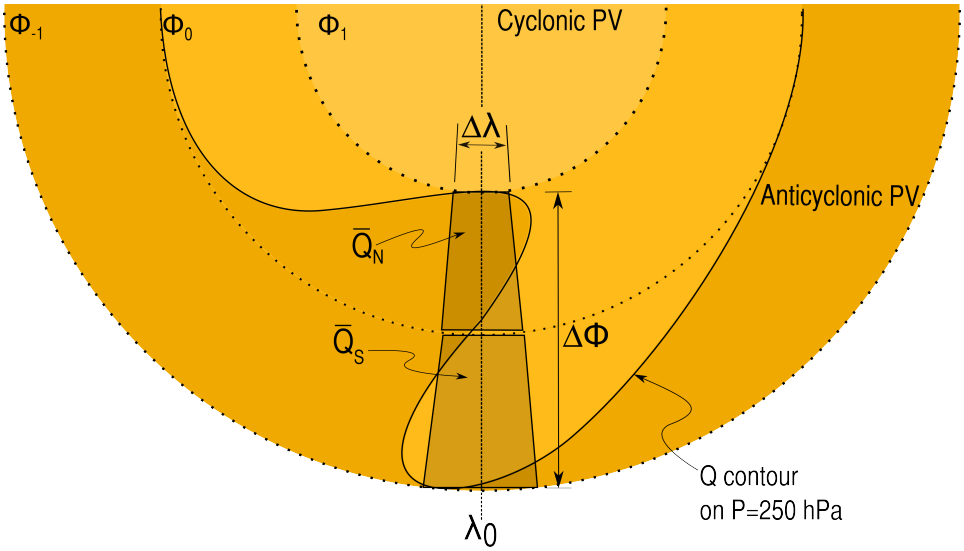

Figure 2.1: Schematic of wave breaking, three selected latitude lines are dashed, with the PV on an isobaric surface shown in colors, darker being more anticyclonic. A selected contour is displayed as a breaking wave that would be identified using the point (ϕ_0, λ_0) and equation 2.1. The two boxes marked A_N and A_S also correspond to equation 2.1.

2.3 SSW detection

To detect major sudden stratospheric warmings, the World Meteorological Organization (WMO) definition was used. The zonal mean zonal wind ($\overline{u}$) at 10 hPa, 60°N transitions from westerly ($\overline{u}$ >0) to easterly ($\overline{u}$ <0) between November 1 and March 31. If a major warming is identified, a second may be identified only after $\overline{u}$ becomes westerly for 20 consecutive days after the first warming central date.

Similar to Quiroz (1986), minor warmings are identified by the zonal mean meridional gradient of temperature from 45°N to 90°N on the 10 hPa surface. This gradient ($\partial T/\partial y$) is normally negative in the winter stratosphere (cold air over the

pole, warm over the tropics). During a warming event this gradient reverses to positive. A minor warming is defined when $\partial T/\partial y$ reverses, but $\overline{u}$ does not within 20 days of the temperature gradient reversal.

2.4 Composites

To generate composites, which are ensemble averages over many events of a particular type, blocking and sudden warming events are identified then blocking events are grouped by their time relative to a sudden warming then by what longitude each is centered on. Three temporal groups were used. In "PRE", the sudden warming event occurs before block onset, for "POST", the sudden warming event occurs at or after block onset, and in "NSW" or non-sudden warming, there is no sudden warming within 10 days of onset or breakdown. The 10 day cutoff was chosen as a reasonable interaction timescale after Martius et al. (2009).

Three geographical sectors were chosen, and blocking events were sorted by which longitude each was closest to: 0°(Atlantic/Europe), 60°W (Greenland), 120°W (Pacific/Asia) which are similar to the sectors described in Woollings et al. (2010). The Atlantic/Europe sector spans 30°W to 120°E, the Pacific/Asia sector spans 120°E to 90°W (150°of longitude each), with the Greenland sector covering the remaining area from 90°W to 30°W, spanning 60°of longitude, illustrated in figure 2.2.

Two types of composite averages were generated: shifted, and non-shifted.

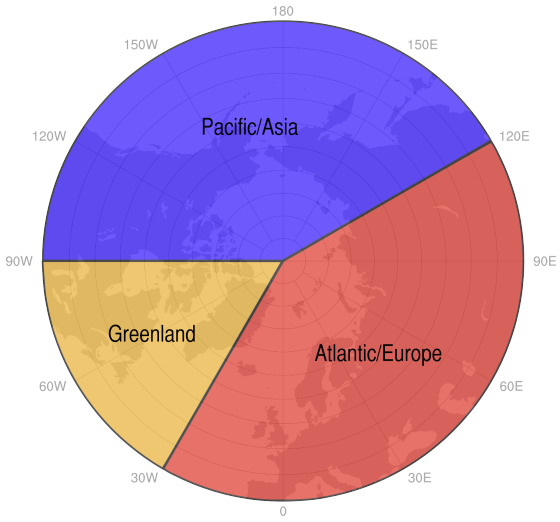

Figure 2.2: Sectors used to distinguish blocking location. Red is 0°(Atlantic/Europe), Yellow is 60°W (Greenland), and Blue is 120°W (Pacific/Asia).

The shifted composite moves the data so that it is centered on the blocking event, meaning the center of the block is at 45°N latitude, and either 0°, 60°W or 120°W longitude depending on the sector in which it occurs. Only data 20°north and south of the blocking center is retained, if the center is further north than 70°, then the center is re-assigned to be 70°N, which occurs in only 17 cases out of 476 for the NCEP data set, with the maximum change being 2 grid points (5°), and does not occur in the MERRA events, with the highest latitude identified being 70°N. The non-shifted composites average the events without re-centering, used in zonal mean analysis. Both composites contain a certain number of days before and after block onset, depending on the variable in question, with the daily variables (u and v wind, temperature, height, and PV) containing 30 days and long time averaged variables (average heat flux and polar cap averaged PV) contain-

ing 60 days.

A second set of composites was generated using the concept of interference with climatology. The relative vorticity ($\vec{\zeta} = \nabla \times \vec{V}$) was calculated on the same pressure level where wave breaking was identified (250 hPa), and the average within a 10°x 10°box surrounding the blocking center was calculated at block onset. This was then repeated for the climatology of the block onset day and if the two values were of matching sign, the block was categorized as a constructive interference block, otherwise the interference was deemed destructive.

As mentioned above, there are many more blocking events than SSW events, thus to determine if any difference in patterns were due to the difference in sample size, a random sample of the NSW blocking events was chosen from the available events. This was done using a pseudo-random number generator whose algorithm is detailed in L'Ecuyer and Côté (1991). The pseudo-random generator produced a number $0 \leq R \leq 100$ for each NSW event; if $R \leq 5$, the event was selected for the random NSW composite, others were discarded, thus selecting approximately 5% of the NSW events for comparison to all NSW blocking events.

2.5 Meridional Heat Flux

The divergence of Eliassen-Palm flux has been used in the study of atmospheric dynamics since Eliassen and Palm (1961) for a variety of phenomena. It represents a flux of wave activity in the zonal-mean sense and is studied on the lat-

itude/vertical plane. In Newman and Nash (2001) and Sjoberg and Birner (2012), only the vertical component of the total flux was investigated, and this was followed here. Equation 2.2 shows that the time rate of change of the zonal mean zonal wind can be approximated by the vertical divergence of the vertical component of E-P flux. Equation 2.3, where f_0 is the Coriolis parameter, R_d the dry gas constant, $\overline{\sigma}$ is the zonally averaged static stability, v is the meridional component of wind, and T is temperature, shows the relationship between F_p and meridional eddy heat flux, with the over-line representing the zonal mean, and the prime departure from it.

$$\frac{\partial \overline{u}}{\partial t} \approx -\frac{\partial F_p}{\partial p} \tag{2.2}$$

$$F_p = \frac{f_0 R_d}{p\overline{\sigma}} \overline{v'T'} \tag{2.3}$$

The heat flux is partitioned into components, as in equation 2.4, where the over-bar indicates zonal mean and the prime represents departure from it, v is the meridional (north-south) component of the wind in $m\,s^{-1}$, and T is temperature in Kelvin. The subscript C indicates long term climatological average and A denotes anomaly from climatology, and again, over-bar indicates zonal mean while prime denotes departure from the zonal mean. The first two right hand side terms of equation 2.4 are the anomaly and total climatology terms respectively, and the final two terms are the interference between climatology and anomaly.

$$H = \overline{v'T'} = \overline{v'_A T'_A} + \overline{v'_C T'_C} + \overline{v'_C T'_A} + \overline{v'_A T'_C} \tag{2.4}$$

As in Sjoberg and Birner (2012), the eddy meridional heat flux was averaged between 45°N – 75 °N on 200 hPa for the non-shifted composites. For the shifted

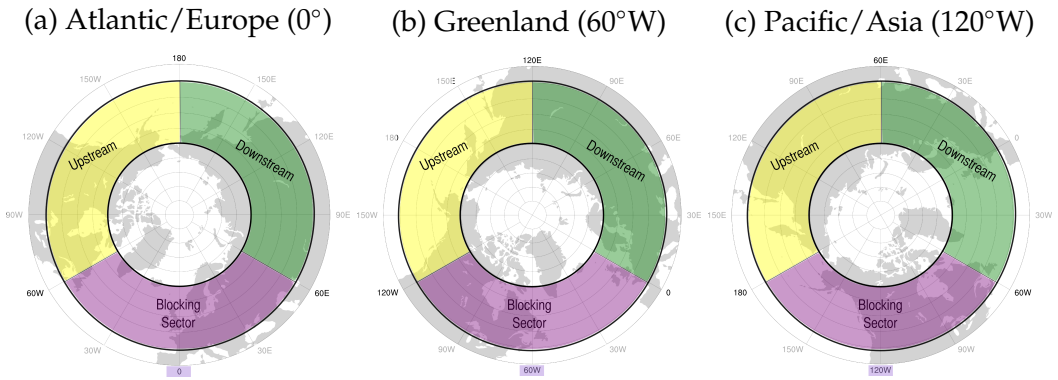

Figure 2.3: Schematic illustrating areas over which heat flux sector averages are taken.

composites, this was adjusted by necessity to 45°N – 65°N, which means the magnitude of non-shifted and shifted composite averages are not to be compared. In addition to the complete zonal average, several smaller sector averages were taken. This was to investigate where the greatest contribution to the total was located. The hemisphere was split into 3 equal sectors of 120°longitude width. The first of which was centered on the block center (thus 60°west, 60°east of center were averaged), then the next 120°downstream, then the previous 120°upstream (given typical west-east midlatitude flow), this is illustrated in figure 2.3, note that these sectors are different from the sectors used to group blocking events. These sector averages are taken relative to each blocking event's center.

The meridional eddy heat flux was also examined for scale variations. This was done first using Fourier filtering in the zonal direction of both the zonal eddy meridional wind component (v') and eddy temperature (T'). At every time, level and latitude, the Fourier coefficients are found for the longitudinal series of v' or T' using equation 2.5, where $f(x)$ is either $v'(x)$ or $T'(x)$, $F(k_x)$ are the complex Fourier coefficients i is $\sqrt{-1}$, e is the base of the natural logarithm, N is the number of points in x, and k_x is the wave number in the zonal direction.

$$F(k_x) = \frac{1}{N} \sum_{x=0}^{N-1} e^{i k_x x} f(x) \tag{2.5}$$

The coefficients outside the desired wave number range are set to 0, and the backward transform is used to generated a filtered field ($\widehat{f(x)}$) using equation 2.6. Here, the wave numbers for planetary scale waves are defined as $k_x \epsilon [0, 3]$ and synoptic scale waves as $k_x \epsilon [4, 8]$.

$$\widehat{f}(x) = \frac{1}{N} \sum_{k_x=0}^{N/2-1} e^{-i k_x x} F(k_x) \tag{2.6}$$

It was performed again using a spherical harmonic based method detailed in Sardeshmukh and Hoskins (1984). It uses Legendre polynomials to transform the wind and temperature data to phase-space, then a truncation is performed and the data are transformed back to real-space. This was done to make the filtering results more robust, as the Fourier method may be subject to ringing when using a square band-pass or low-pass filter.

2.6 Ertel's Potential Vorticity

An additional method of differentiating blocking events associated with sudden stratospheric warmings from those that are not was developed by Colucci (2013), who found that the tendency of polar-cap (defined as 60°– 90°N) averaged Ertel's PV on the 30 hPa surface was more anticyclonic during selected blocking events associated with SSWs when compared to selected blocking events with no associated SSW, though this is an indicator rather than a predictor. Ertel's PV is defined in equation 2.7, where g is acceleration due to gravity, η is absolute vorticity (defined as $\zeta + f$ where ζ is the curl of the horizontal wind $\nabla \times \vec{V}$ and f is the Coriolis parameter), θ is potential temperature, and u and v are the zonal and meridional components of the wind, respectively. With vertical coordinate p, pressure, and horizontal coordinate x in the zonal direction, and y in the meridional direction. The units of Q are $K\,m^2\,kg^{-1}\,s^{-1}$, with a PV unit, or PVU, defined as $10^{-6} K\,m^2\,kg^{-1}\,s^{-1}$.

$$Q = -g\left[\eta\frac{\partial\theta}{\partial p} + \frac{\partial u}{\partial p}\frac{\partial\theta}{\partial y} - \frac{\partial v}{\partial p}\frac{\partial\theta}{\partial x}\right] \tag{2.7}$$

Here an adaptation of this calculation is used; tropospheric (200 hPa) polar-cap averaged EPV is averaged over 10 days rather than using the time rate of change in the stratosphere, as this project is concerned with the troposphere's effects on the stratosphere.

CHAPTER 3

BLOCKING STATISTICS

3.1 Frequency and Geographic Distribution

As mentioned above, blocking events are far more frequent than sudden stratospheric warmings. Figure 3.1 illustrates that while every year has 4 or more blocking events, there are multiple years without a major SSW. Notable is 1994–1995, with 16 blocking events but no major warming.

Figure 3.2 shows that there are many more events in the NSW group than PRE and POST. Interestingly, though the Greenland (60°W) sector is the smallest (fig. 2.2), there are relatively more SSW associated blocking events compared to the Pacific/Asia sector in the NCEP dataset even though there are fewer total blocking events in the Greenland sector, though this is not the case for MERRA. The same assessment is repeated in figures 3.3 and 3.4 for minor and all warmings respectively. The same geographic distribution is not replicated when minor warmings are factored in, the two larger sectors have more events across all categories, with non-warming associated events remaining the largest by far. It should also be noted here that the higher resolution MERRA data results in a larger number of blocking events per year identified, which was tested by interpolating MERRA data to the NCEP grid via spherical harmonics, resulting in similar frequencies for the years in common (1980-2010).

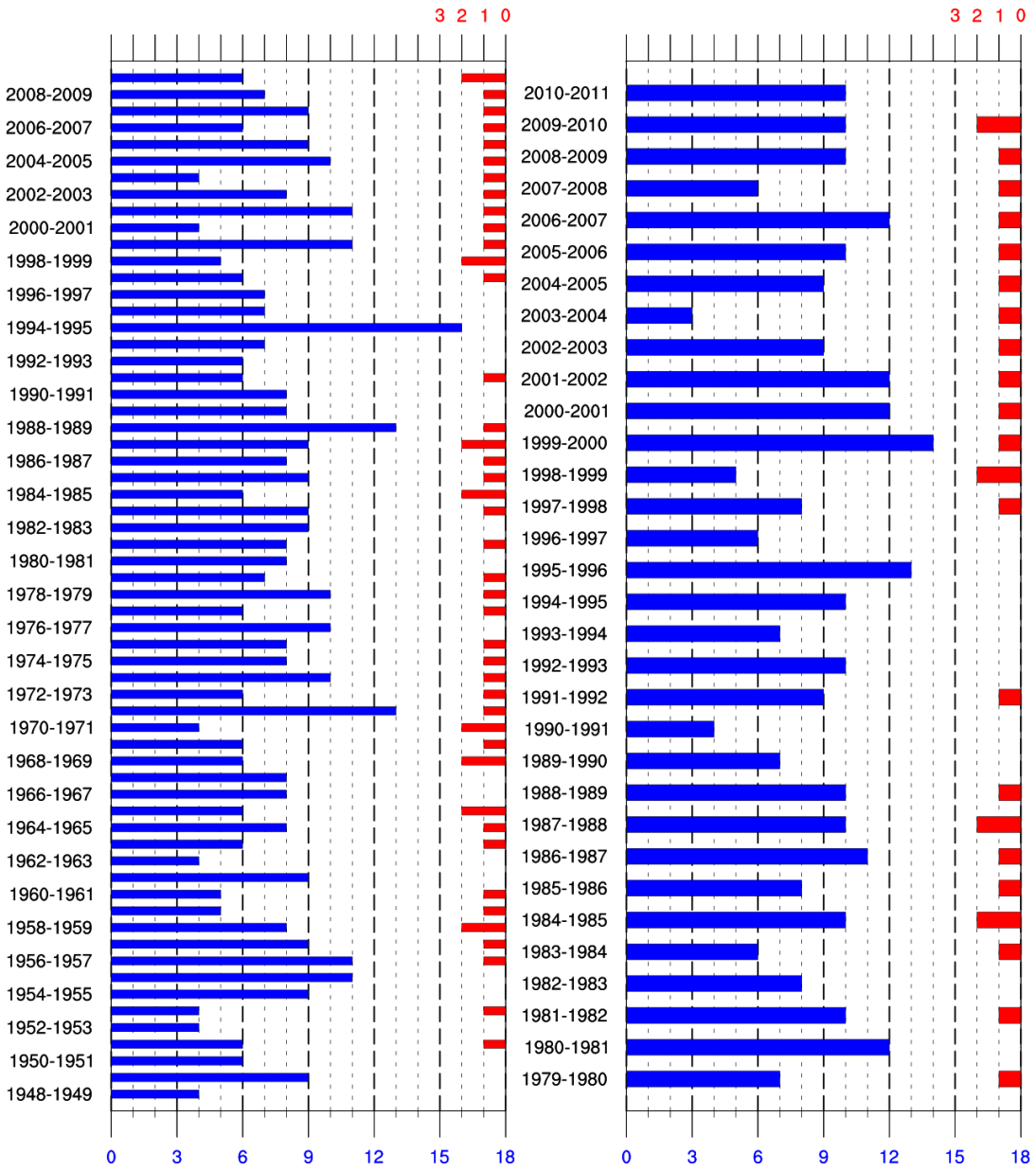

(a) NCEP (1948-2010) (b) MERRA (1979-2011)

Figure 3.1: Number of blocking and major SSW events by year. Length of blue bar indicates number of blocking events on the bottom axis, length of red bar indicates number of major SSW events on the top axis. Where no red bar appears, there are no SSW events that year. (e.g. 1979-1980 there are 7 blocking events and one SSW event in both data sets). For (a) NCEP data is used spanning 1948-2010, and in (b) MERRA data is used spanning 1979-2011.

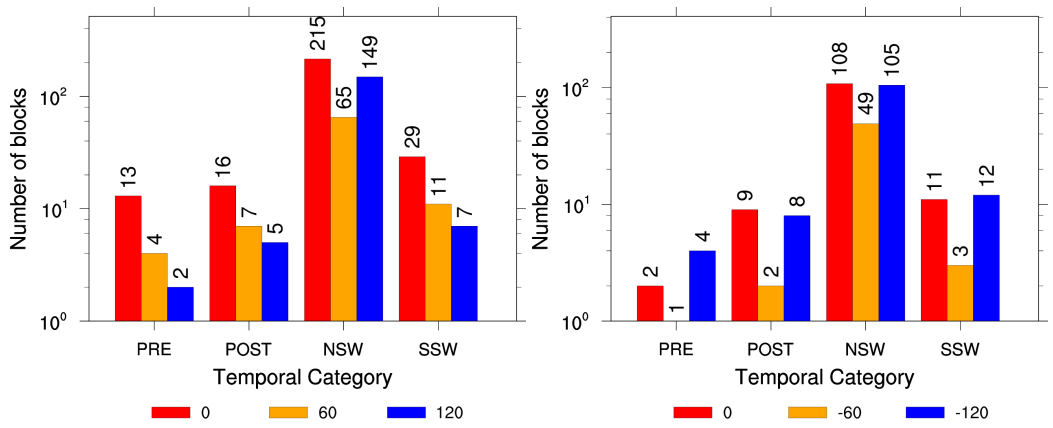

(a) NCEP (1949-2010) (b) MERRA (1980-2011)

Figure 3.2: Blocking frequency by temporal group and sector for major warmings. PRE group for SSW event occurring before blocking event, POS group for SSW event occurring after blocking event, NSW group for blocking events without an SSW occurring within 10 days of onset or breakdown, and SSW group combining PRE and POS. In (a) events are in NCEP reanalysis for 1949-2010, and in (b) events are in MERRA for 1980-2011. Y-axis is log scale.

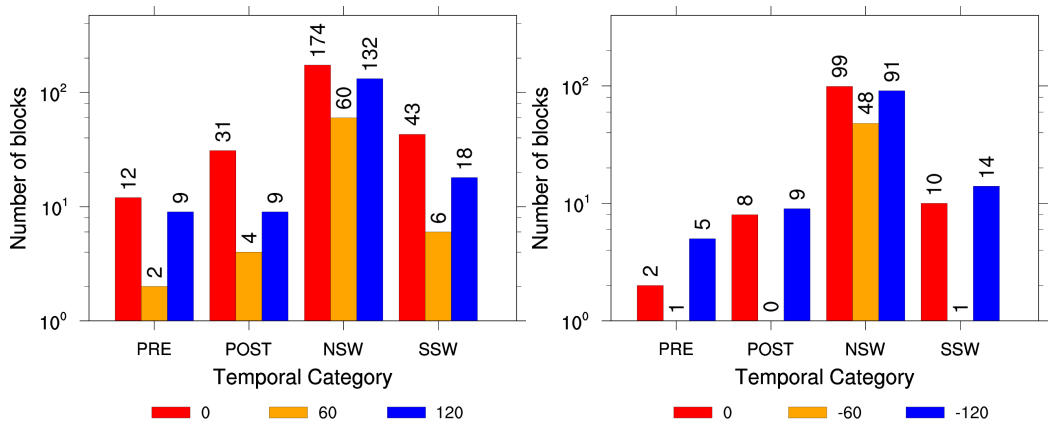

(a) NCEP (1949-2010) (b) MERRA (1980-2011)

Figure 3.3: As in 3.2 but for minor warmings.

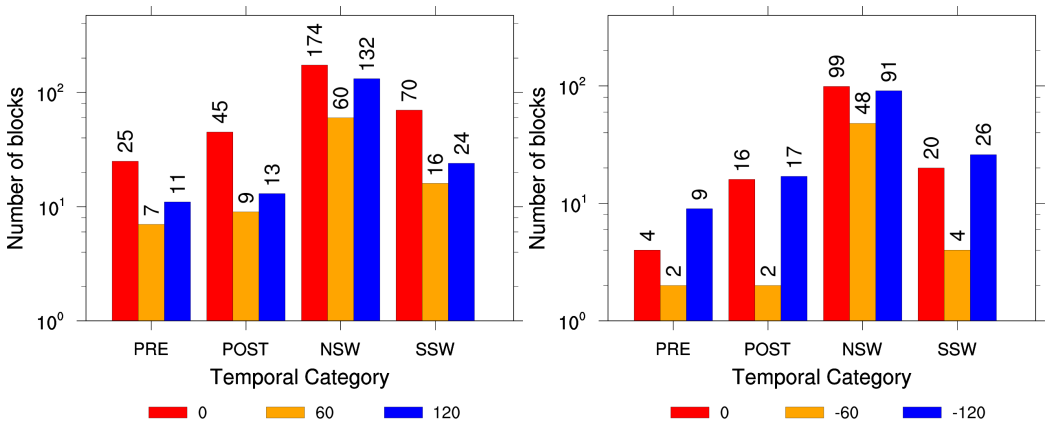

(a) NCEP (1949-2010) (b) MERRA (1980-2011)

Figure 3.4: As in 3.2 but for all warmings.

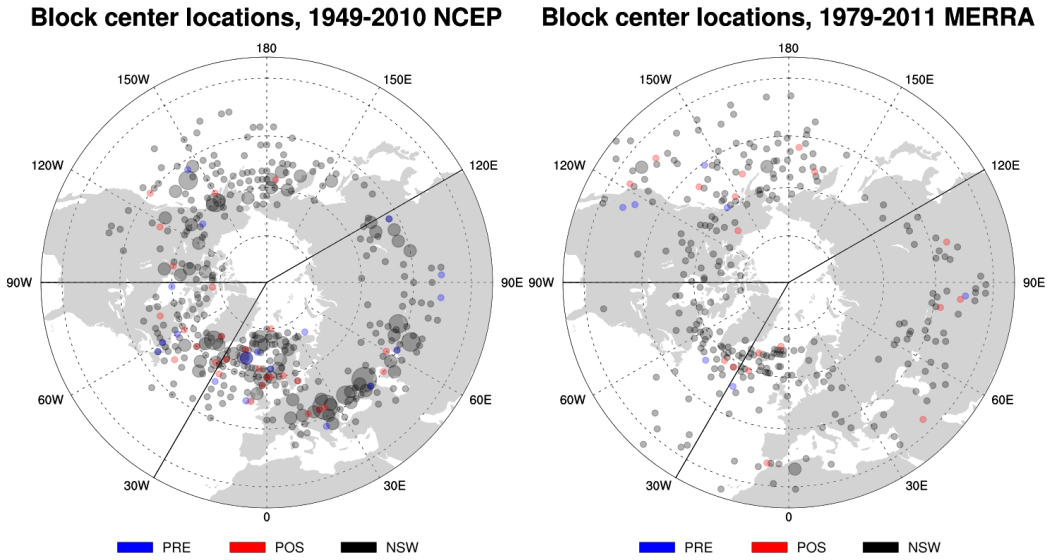

(a) NCEP (1948-2010) (b) MERRA (1979-2011)

Figure 3.5: Blocking event center locations for (a) NCEP and (b) MERRA. Times relative to major warmings indicated by colors. Dark longitude lines indicate sectors. Sizes of circles are frequency of events at each location, larger circles indicate more events.

From figure 3.5, a clustering of events in the Pacific and Atlantic basins with sparse distribution over the continents is seen in both datasets, though southern Europe presents a secondary cluster. Though some clustering exists, there does not appear to be a larger statistical relationship between the longitude of a blocking event and occurrence/non-occurrence of an SSW event.

LON	0	-60	-120
PRE	30.000	-66.250	-138.750
POS	7.812	-55.357	-136.000
NSW	30.942	-53.577	-153.809
SSW	17.759	-59.318	-136.786
PRE-NSW	0.057	0.873	0.899
POS-NSW	0.998	0.201	0.751
SSW-NSW	0.917	0.703	0.872

Table 3.1: Above double line: average longitude center for major warming associated/non-associated events. Below double line: P-Values of one sided Student's t-test for unequal variances for differences in block longitude between groups indicated in left column of each row, in sectors indicated in each column. Values greater than 0.9 are regarded as significant.

From table 3.1 the SSW associated events in the larger sectors appear to be more significantly different from the NSW blocking events than in the smaller Greenland sector, with the differences being most significant for post-block SSWs (POS) in the Atlantic/Europe sector. The same is repeated for MERRA, though there are fewer events; thus for the Greenland PRE group, a t-statistic is unable to be generated. Significance is seen in the difference between PRE and NSW blocking events in the Pacific/Asia sector, as well as POST and NSW and SSW/NSW

LON	0	-60	-120
PRE	28.750	-46.875	-129.062
POS	26.736	-36.250	-61.250
NSW	26.528	-53.508	-80.899
SSW	27.102	-39.792	-83.854
PRE-NSW	0.035	—	0.999
POS-NSW	0.010	0.997	0.301
POS-PRE	0.031	—	0.800
SSW-NSW	0.028	0.980	0.066

Table 3.2: As in table 3.1, but for MERRA data

in the Greenland sector. The same process was replicated for all warmings, without significant differences in longitude center averages. In addition, the latitude centers for all warmings were tested, and again no significant differences were seen with the average latitude across sectors and groups around 55-60°N, thus as stated before, a larger statistical relationship is not apparent between longitudinal location of blocking events and SSW occurrence.

3.2 Block duration

As the duration of heat fluxes has been shown to be related to SSW occurrence (Sjoberg and Birner, 2012), the average duration of blocking events were tested dependent upon blocking event group and sector. In the NCEP dataset (fig 3.6a), major warming POST events are significantly (α = 0.05 or 95% confidence) longer on average than NSW in the Atlantic/Europe sector. On average the SSW cate-

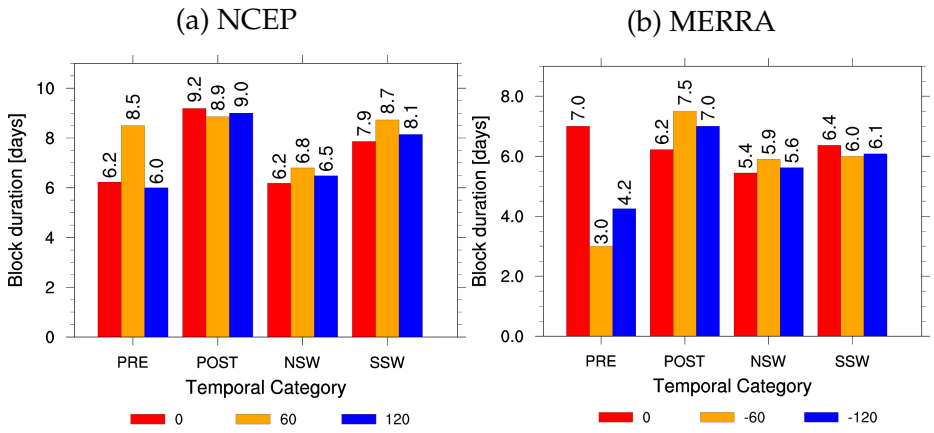

Figure 3.6: Average blocking event duration (Calculated by the final date of blocking event definition satisfaction minus onset date) sorted by sector and group relative to major warmings.

gory events in all sectors are longer than NSW blocking events, though it is only significant ($\alpha = 0.1$) in the Atlantic/Europe sector. For all warmings, (figure 3.7a) with significant differences ($\alpha = 0.1$) in the Atlantic/Europe and Pacific/Asia sector between POST and NSW events, as well as the overall SSW average in the Pacific/Asia sector.

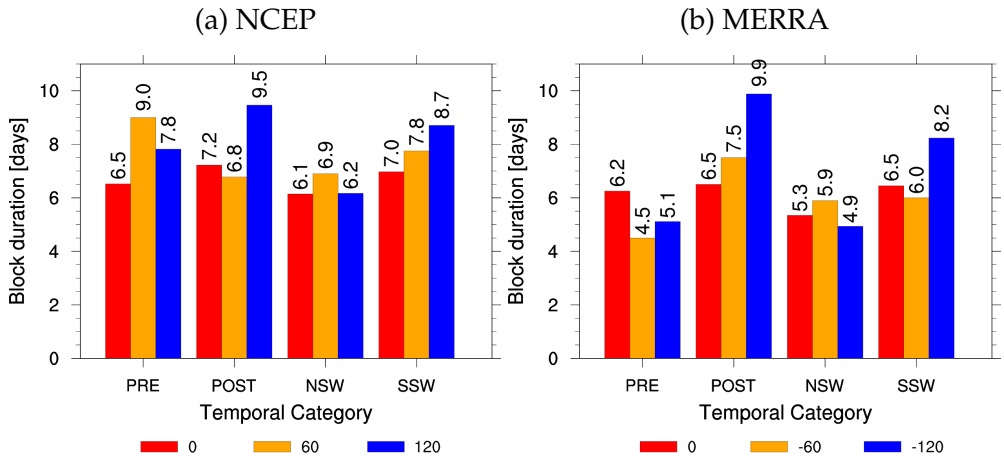

Figure 3.7: As in figure 3.6 but relative to all warmings

The MERRA dataset events have a similar pattern. For major warmings (fig 3.6b) the POST blocking events in the Atlantic/Europe sector are significantly longer ($\alpha = 0.1$), as are the SSW category events. For all warmings (fig 3.7b), the POST blocking events are again significantly longer than the NSW category events in both Atlantic/Europe and Pacific/Asia sectors, as are the SSW category events in the Pacific/Asia sector.

CHAPTER 4

COMPOSITES: GROUPED BY SECTOR IN NCEP/NCAR REANALYSIS

4.1 Synoptic Overview

Blocking events typically have a recognizable geopotential height signature, a large mid-tropospheric ridge or cutoff high/low dipole structure. The typical blocking event ridging pattern in all Atlantic/Europe composites, with the trough being most pronounced in the POST composite can be seen in figure 4.1. The NSW composite in this sector lacks other synoptic waves outside of the blocking region, though with a selection of random NSW events (fig. 4.2) this difference is not apparent. Synoptic waves of similar amplitude and wavelength can be seen in all three group averages.

The Greenland PRE composite also features an amplified ridge; though it is east of the central longitude; in addition, a secondary amplified ridge is observed west of the central longitude. Interestingly, the typical blocking signature is not seen in the POST composite, though there exists slight ridging within the blocking region. The NSW composite features a dipole pattern, with a second trough 180°removed from the blocking ridge. The Pacific/Asia composites look similar to the Atlantic/Europe composites, though with only two events in the PRE composite the field is considerably nosier.

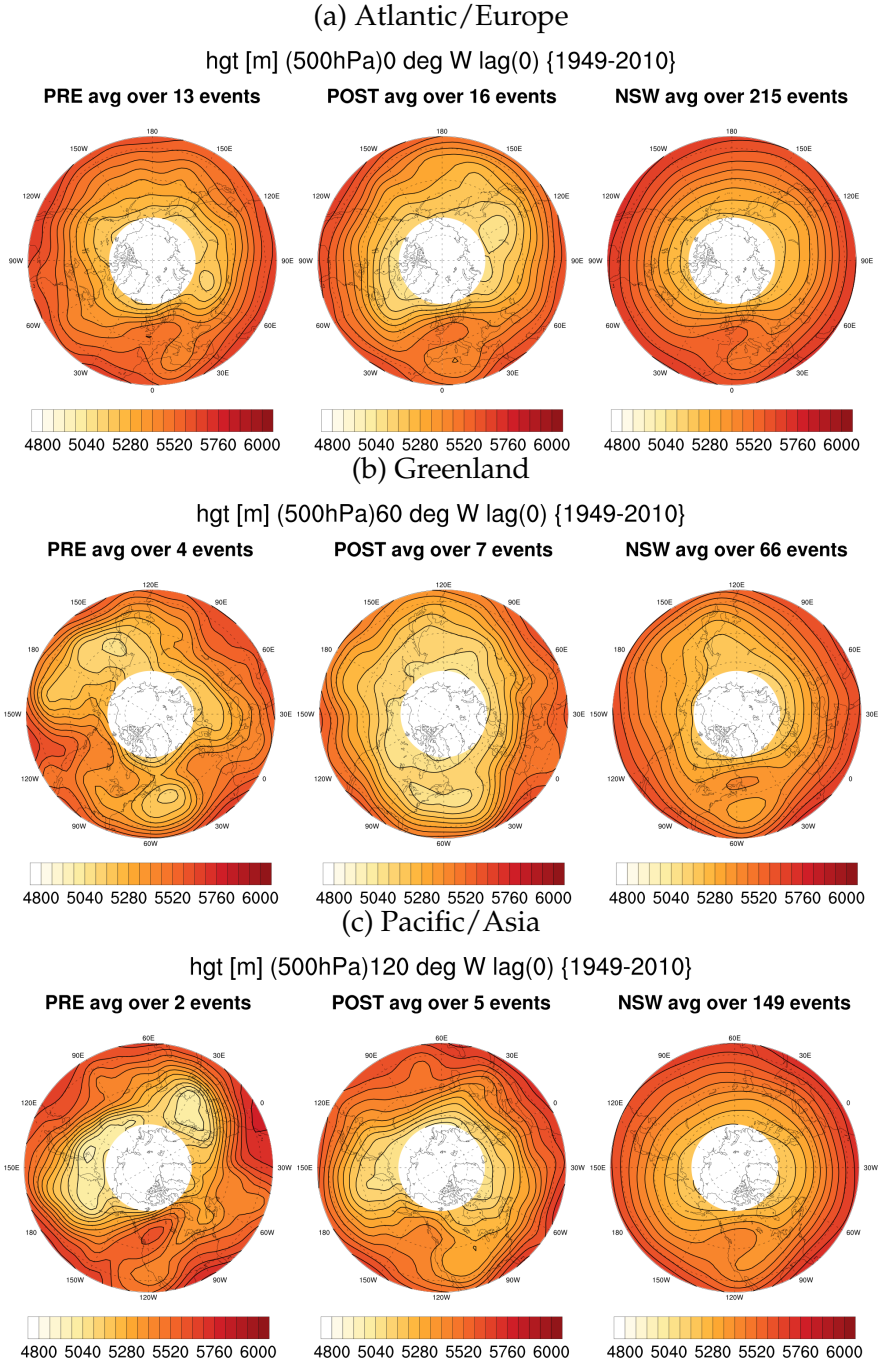

Figure 4.1: Composite average geopotential height at 500 hPa in meters at block onset for each group in (a) 0°W, (b) 60°W, and (c) 120°W. PRE events in the left column, POST in the center, NSW right.

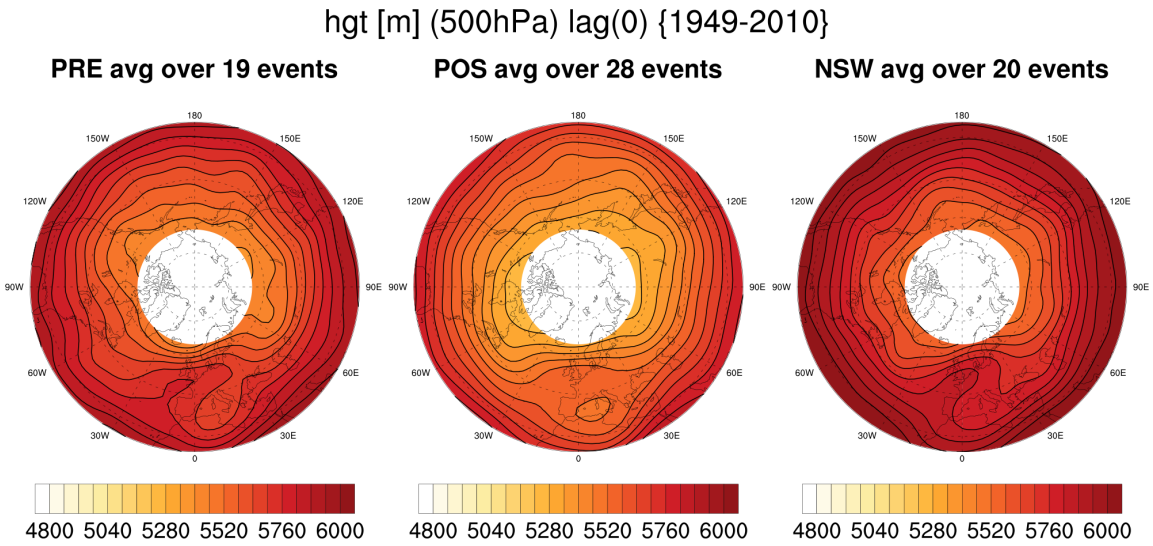

Figure 4.2: Composite average geopotential height at 500 hPa in meters at block onset for each group PRE events in the left column, POST at center, randomly selected NSW events at right.

4.1.1 Aleutian High

Previously associated with SSWs (Harvey and Hitchman, 1996), the Aleutian High is an anticyclonic feature in the stratosphere over the Aleutian archipelago, it is defined by a closed anticyclone near 165°W, 65°N. Figure 4.3 shows this the Aleutian High signature in both PRE and POST composites, and absent in the NSW composite. Note that heights are higher in both the PRE and POST cases within the polar stratospheric vortex. This difference in signature is also present for a composite of randomly selected NSW blocking events, where no closed anticyclone is present over the Aleutians, indicating that this is an actual signature of SSW associated blocking events. Though it should be noted that the Aleutian high

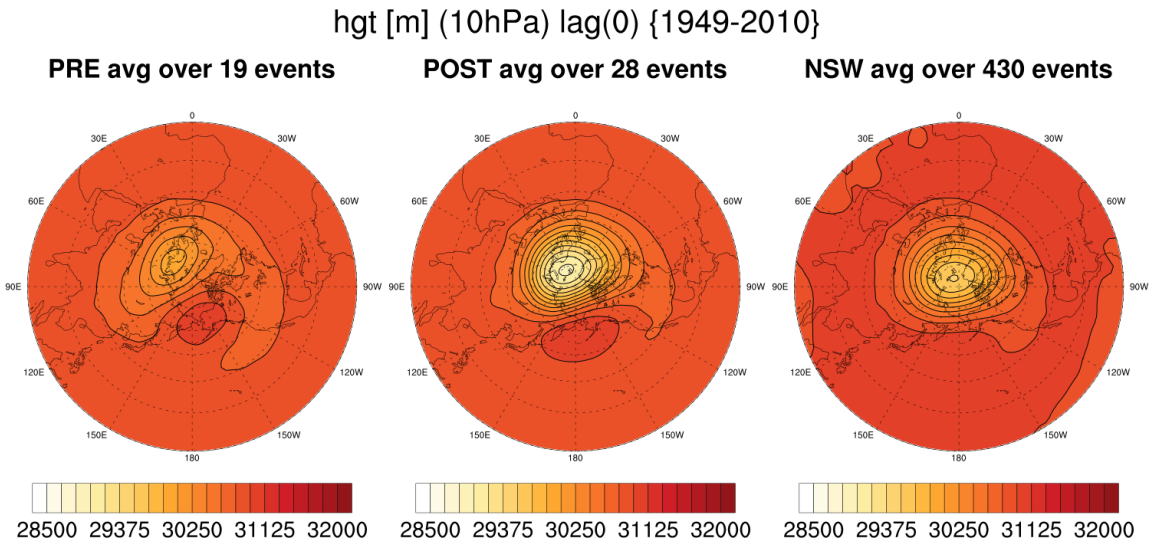

Figure 4.3: Composite of geopotential height on 10 hPa surface in meters at block onset for each group (regardless of sector) with PRE events in the left column, POST in the center, NSW right.

is an indicator rather than a predictor, as it does not appear significantly before the SSW event.

4.1.2 Potential Vorticity Evolution

The PV field evolution shown in figure 4.4 illustrates the locations of anticyclonic and cyclonic climatological anomalies over time relative to the block onset location. This is useful in determining whether or not the origin of the anticyclonic anomaly plays a role in differentiating blocking events with and without SSWs.

Starting with the Atlantic/Europe sector, the PRE composite is interesting in

that the anticyclonic anomaly is much smaller in longitudinal extent and short lived than in other cases. It can be seen both west and east of 0°(note that 0°is split on the diagram) but is only present within a few days of onset. The POST composite features a large anomaly spread over approximately 14 days and is fed by an anticyclonic anomaly from half a hemisphere upstream nearly 20 days in advance of the block onset.

The Greenland sector composites greatly aid in understanding the events, because as mentioned above, there is no prominent geopotential height blocking signature in the SSW composites. There is, however, an anticyclonic PV anomaly that is present nearly 10 days in advance of block onset, in the PRE composite, that retrogresses toward the block onset center, which then stays in place for approximately 11 days. In the POST composite, the anticyclonic anomaly progresses (as in the Atlantic/Europe composite) though it is only present approximately 10 days in advance, and has a lesser longitudinal extent. Also notable here is the presence of a second anomaly centered near 30°E that is present 20 days before onset and stays in place for approximately 6 days after onset. The NSW composite also features an anticyclonic anomaly that retrogresses slightly from around 5 days before onset and persists weakly up to 20 days after onset, with only weak anomalies outside the blocking region. In the Pacific/Asia composites, less PRE events are available, thus the physical significance of that composite is debatable. Though both PRE and POST composites feature an anticyclonic anomaly that largely develops in place, though in the PRE composite it is featured 20 days before onset in the same region. The NSW composite again features fewer anomalies elsewhere;

here the anticyclonic anomaly is present approximately 9 days before onset, and is present 20 days after onset.

To determine whether or not the climatological PV anomalies of the SSW associated events are statistically different from those of the non-associated events a Student's t-test was performed (fig. 4.4). In the Atlantic/Europe composites, the PRE composite features no significantly different PV anomaly in the blocking region near onset, but does have a significant cyclonic anomaly in advance of and at onset 180°upstream. The POST has some significantly greater anticyclonic PV near the time of onset near the block center, in addition to significantly greater cyclonic PV 180°upstream of the center just after onset. Both also feature small pockets of significance outside the blocking sector distributed through time. Neither Greenland composite has significant anomalies in the blocking region near onset time. The POST composite is more anticyclonic between 0°–30°E before and just after onset with some significance. In the Pacific/Asia sector, both PRE and POST composite averages lack significant differences in the blocking region.

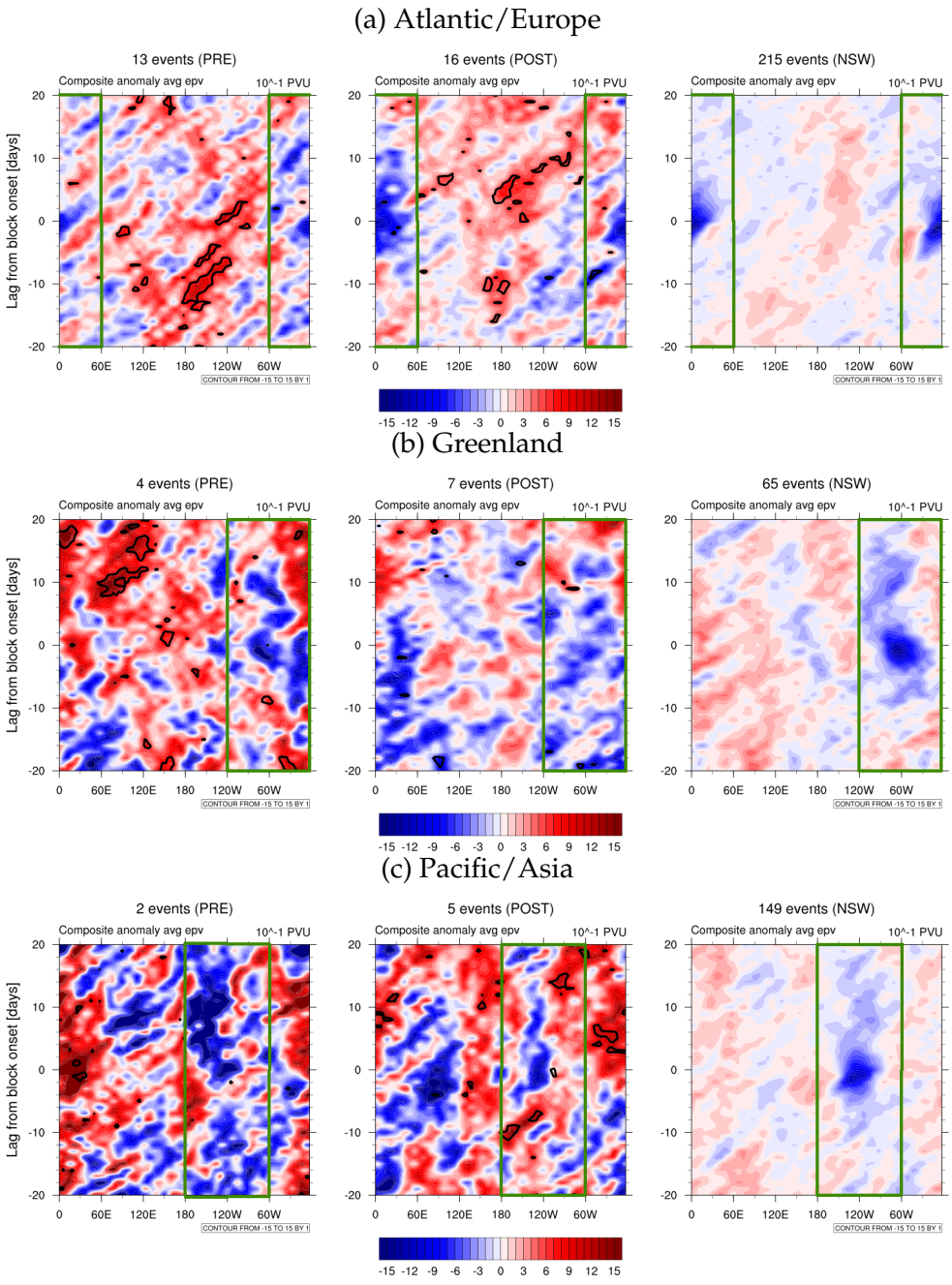

Figure 4.4: Composite evolution of the anomaly from climatological PV at 200hPa over time relative to block onset (day 0), averaged between 45-60°N in (a) 0°W, (b) 60°W, and (c) 120°W. PRE events in the left column, POST in the center, NSW right. Contoured is statistical significance to 90% confidence, blocking event region shown with green box.

4.1.3 U-wind

An obvious distinction between the SSW and NSW composites is the zonal mean zonal wind at 60°N, 10 hPa, by definition. However, there may be other levels on which there is a difference in the zonal mean zonal wind (fig. 4.5). The Atlantic/Europe PRE composite features a weakened upper tropospheric $\overline{u}$, followed by a weakened stratospheric $\overline{u}$, which is then followed by a weakening of the tropospheric $\overline{u}$. This can be compared to the Pacific/Asia composite, where there is a primary weakening of $\overline{u}$ in the stratosphere, followed by a weakening in the troposphere. The Greenland composite is a completely different story, as it features anomalous easterlies throughout the troposphere and stratosphere before, during, and after onset, though the anomalous tropospheric easterlies are reduced 10 days after onset.

(a) Atlantic/Europe

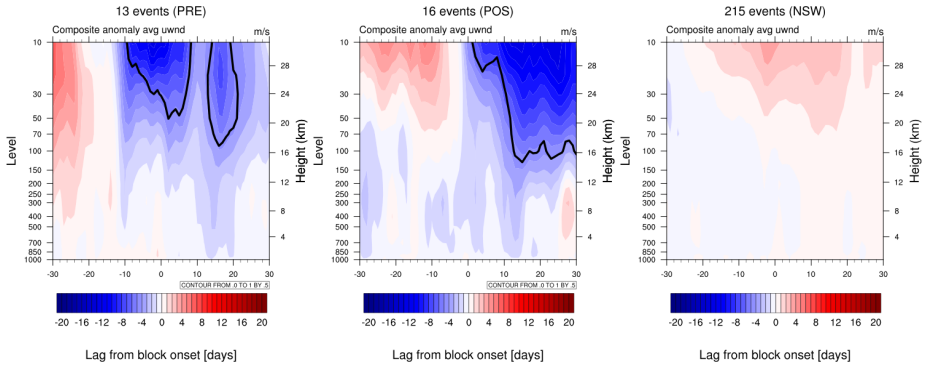

(b) Greenland

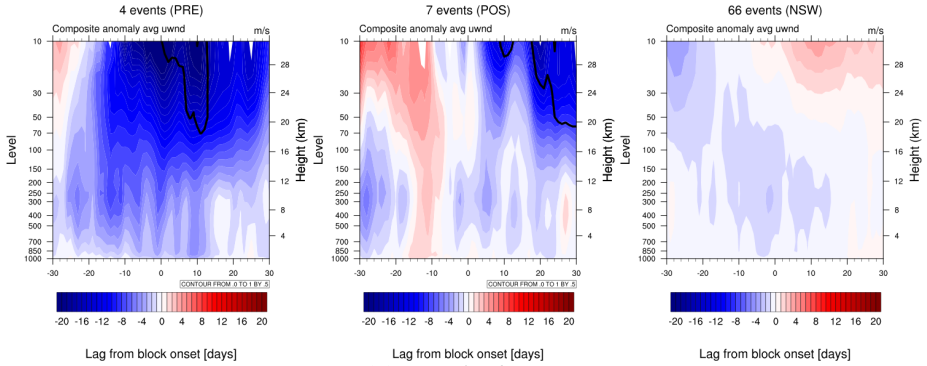

(c) Pacific/Asia

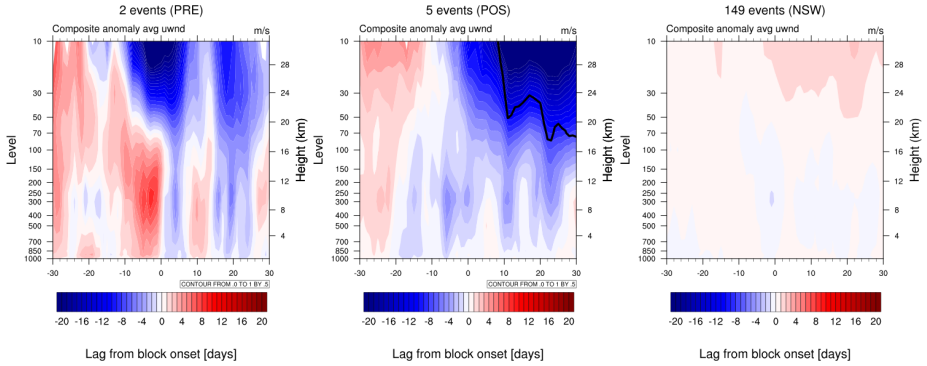

Figure 4.5: Evolution of composite climatological anomaly zonal mean zonal wind on height vs. time plane averaged from ±5°of block latitude center for (a) 0°W, (b) 60°W, and (c) 120°W, with PRE at left, POST in the center and NSW at right. Statistically significant differences between PRE from NSW and POST from NSW to $\alpha = 0.1$ are shown in contours on the left and center panels respectively.

The POST composites, however, share a common theme. There are anomalous $\overline{u}$ westerlies in the stratosphere, at least 30 days before block onset, which end approximately 10 days before onset, transitioning to climatology, or weakly anomalous easterly. The troposphere features an anomalously easterly $\overline{u}$ between 5–10 days before onset, which then appears to connect to the stratosphere just after block onset, when the stratospheric easterlies intensify, and also features a downward connection several days after block onset. The differences of the PRE and POST composites from the NSW composite all feature statistical significance ($\alpha = 0.1$) in the stratosphere just before and after block onset, with no statistical significance in the troposphere with the exception of the Pacific/Asia PRE composite.

4.2 Meridional Heat Flux

4.2.1 Major Warmings

As stated above, Sjoberg and Birner (2012) found a link between the tropospheric meridional eddy heat flux and sudden stratospheric warmings, both major and minor. The patterns match well with expectation here, with significantly larger values associated with the two SSW composites, and the signal mostly from the anomaly, and magnitude from climatology. The PRE composite has its peak spread over day -12 to day -6 relative to block onset with statistical significance

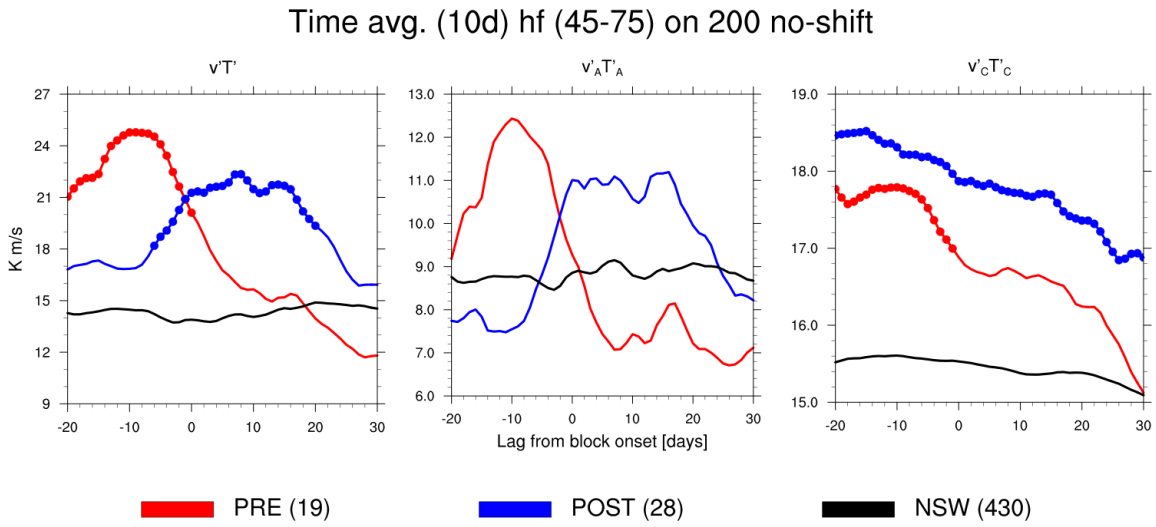

Figure 4.6: Ten day averaged meridional eddy heat flux, averaged over all sectors within each group. Red line indicates PRE, blue is POST, black is NSW. Subscript "C" means climatology component, subscript "A" is anomaly from climatology. Left panel is full eddy heat flux, center panel is anomaly, right is climatology, corresponding to the left hand side of eqn. 2.4 and the first two terms on the right hand side respectively. Dots on PRE and POST curves indicate statistically significant differences from NSW curve to $\alpha = 0.05$.

from day -20 to day 0, while the POST composite has a broader peak that starts near day 0, and ends around day 16 with statistically significant differences from day -6 to day +20. The climatology indicates that the SSW associated blocking events occur when there is climatologically larger heat flux compared to the NSW events and is significant before onset in the PRE composite average, and for the entire POST composite average. Not shown are the interference terms, as they are an order of magnitude or more smaller than the non-interference terms.

Again a random selection of NSW events were used, and is compared to the PRE and POST composite averages in figure 4.7. It can be seen that there is very

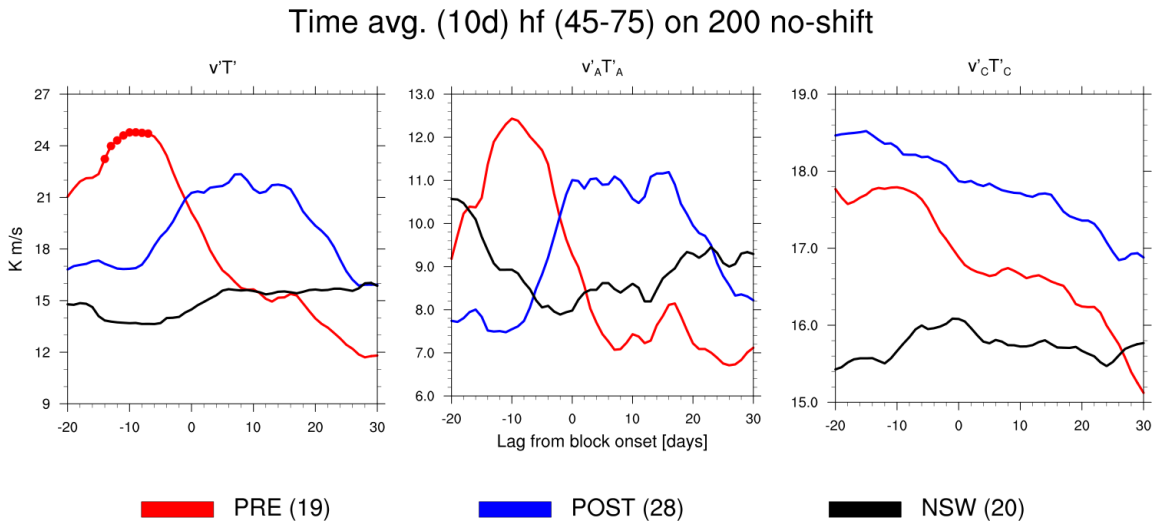

Figure 4.7: As in figure 4.6 but for randomly chosen NSW events and $\alpha = 0.1$.

little difference in the total field from the total NSW composite. The main point here, however, is that the NSW composite heat flux is still less than that of either the PRE or POST composite averages, though it is not statistically significant due to the low number of events. In the interest of examining the geographic origin of the heat flux, each composite was split into three sectors: the blocking sector, centered on the block longitudinal center, the upstream sector to the west of this, and downstream to the east of it as detailed in section 2.4. It is seen in figure 4.8 that in the Atlantic/Europe composite, during the lead up to block onset, the downstream sector average is significantly greater in the full field ($\overline{v'T'}$) in the PRE composite, when compared to its NSW counterpart. At day +10 the POST composite average in the blocking sector features a single point of statistical significance and is greater than its NSW counterpart, while the average in the upstream sector is significantly smaller. The climatology field is significantly greater for the

blocking sector in the POST composite average for day -20–+15 when compared with the NSW average, and the upstream climatology significantly less than the NSW upstream climatology for day -12–+30. No significant differences are seen in the anomaly field in the Atlantic/Europe composite.

In the Greenland composite features significantly greater PRE composite average in the upstream sector from day -20– -13, while the blocking sector average is significantly less in the POST composite average compared with its NSW counterpart near the same time period. Significantly greater climatological heat flux is seen in the PRE composite average in both the external sectors (upstream and downstream) for nearly the entire composite time period, while the only significant anomalies come from the POST composite average in the blocking sector being significantly less than its NSW counterpart.

The Pacific/Asia composite average features significantly greater heat flux in the upstream sector sporadically between block onset (day 0) and day +20, with no significant differences in the PRE composite average full heat flux. The climatological component of the heat flux is seen to be significantly greater in the POST composite average during days +15–+30 in the upstream sector compared to the NSW composite average, while it is significantly less in both PRE and POST composite averages in the blocking sector for days +4–+12 and -10–+1 respectively.

(a) Atlantic/Europe

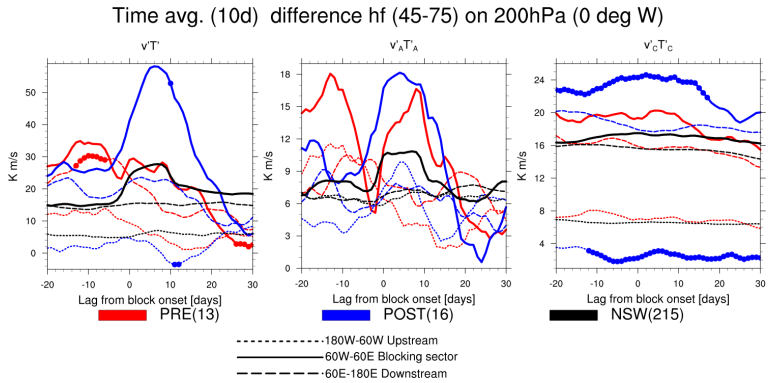

(b) Greenland

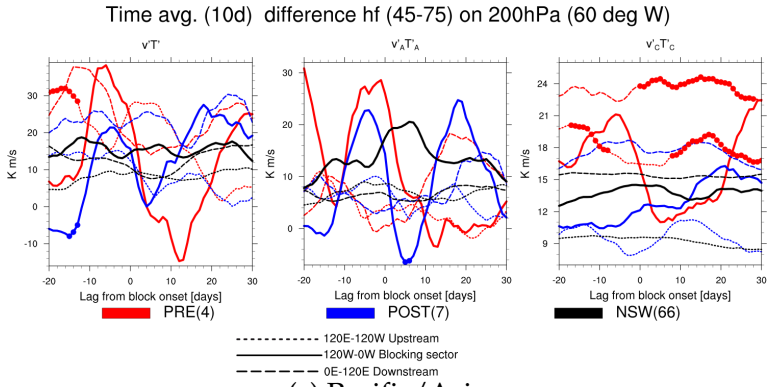

(c) Pacific/Asia

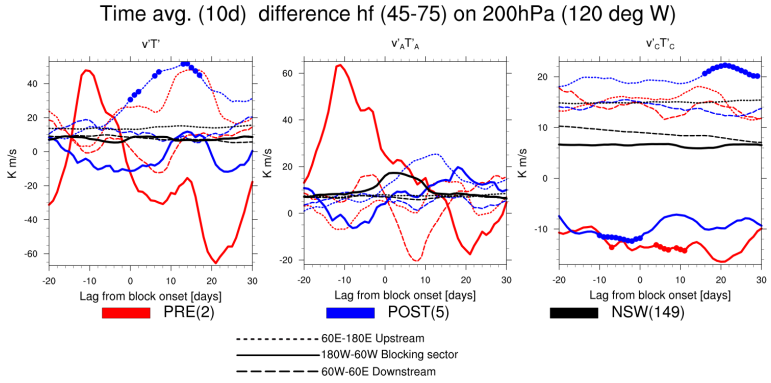

Figure 4.8: Composite sector averaged heat fluxes for (a) 0°W, (b) 60°W, (c) 120°W. Blocking sector is thick solid line, dot-dashed is upstream, dotted is downstream, with red denoting PRE, blue denoting POST and black for NSW. Subscript C denoting climatology, subscript A denoting anomaly from climatology. Significant differences (to $\alpha = 0.1$) between PRE and POST from NSW are indicated with dots for each sector average.

4.2.2 Minor Warmings

These findings have also been investigated comparing blocking events to minor warmings to increase sample size. The group average heat flux (fig. 4.9) has similarities to the group average heat flux for major warmings, though here the peaks are of lower magnitude than in the major warming composites, and also narrower. The POST composite average is significantly greater than the NSW composite average during the entire composite time period, with the PRE composite average is significantly greater near block onset from day -9–+3, and again during days +17–+19. Both PRE and POST climatological components are significantly greater than the NSW climatological component for nearly the entire composite time frame.

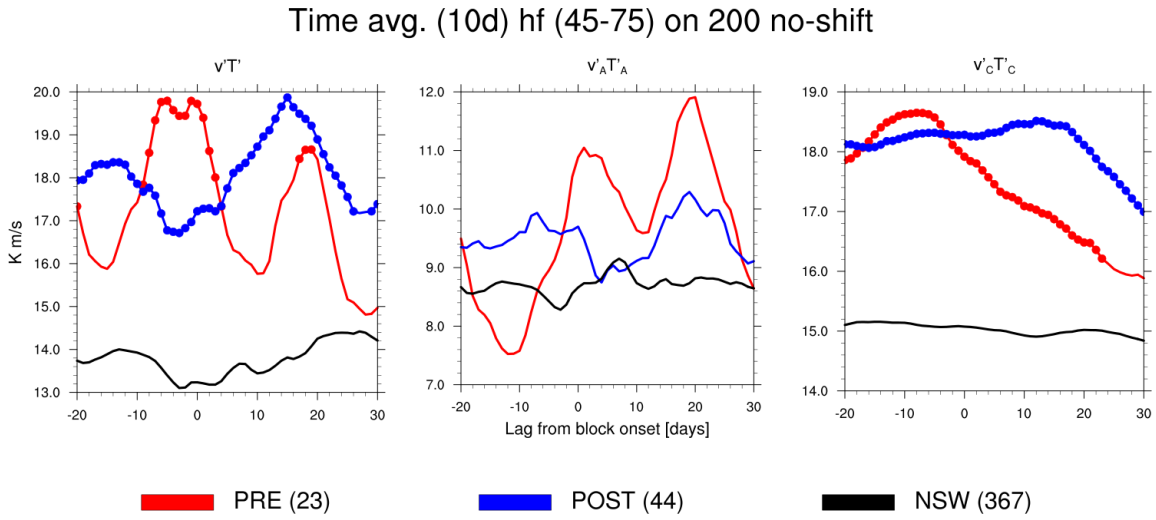

Figure 4.9: As in figure 4.6 but for minor warming associated blocking events.

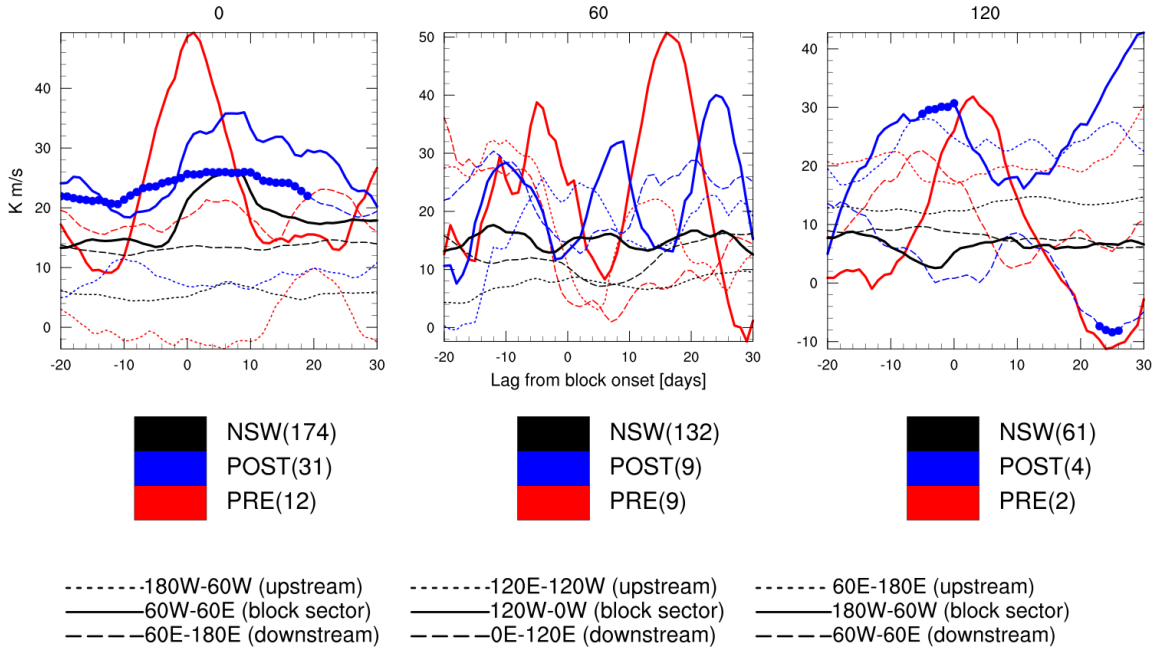

Figure 4.10: Ten Day averaged heat flux, for Atlantic/Europe (left), Greenland (center) and Pacific/Asia (right) sectors. As in figure 4.8, but only full heat flux average is shown for minor warming associated blocking events.

The sector averages, (figure 4.10), also indicate a similar but not identical pattern. In the Atlantic/Europe composite, the blocking sector in the POST composite average is mostly dominant for the entire time period, though only the upstream sector is significantly greater than its NSW counterpart. The PRE composite average in the blocking sector peaks before onset, though it is not significantly different from the blocking sector in the NSW composite average.

The Greenland sector composite for minor warmings does not have any statistically significant differences between PRE and POST sector averages and NSW sector averages, though it appears that for all composite averages, all sectors contribute positively to zonal mean wind deceleration.

Composites in the Pacific/Asia sector are complicated by the lack of events, but do feature significantly larger blocking sector averaged heat flux in the POST composite average near block onset. External sector contributions are not significantly different from their NSW counterparts in either PRE or POST composite averages.

Grouping blocking events associated with both major and minor warmings

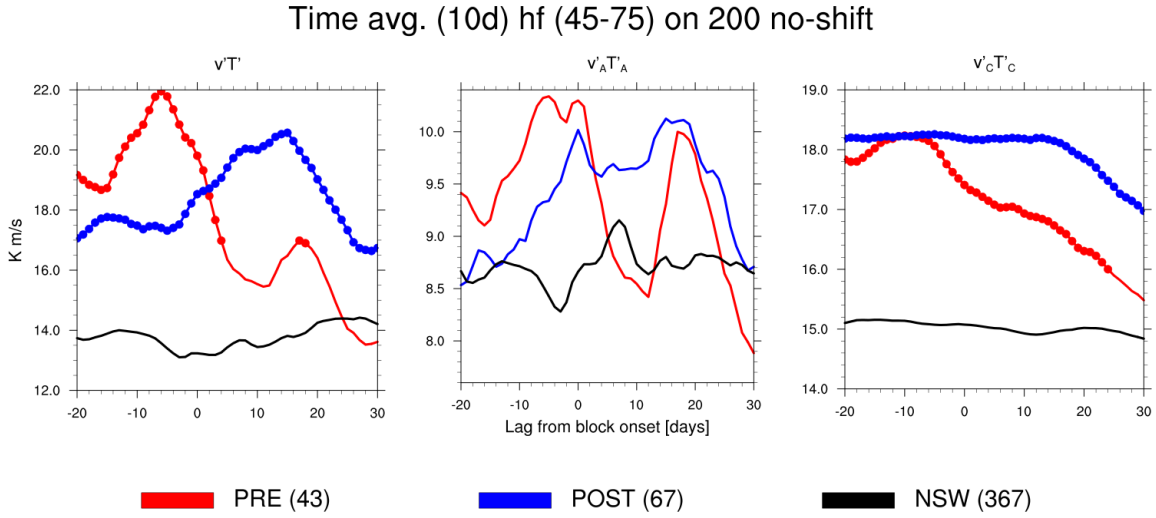

Figure 4.11: As in figure 4.6 but for all warming associated blocking events.

together, the resulting composite (figure 4.11) appears similar to both major and minor composites (fig. 4.6, 4.9 respectively). There is a narrow, large magnitude peak in the full PRE composite before block onset, with a smaller peak following onset, and a broad peak in the full POST composite from days -2–+20. The main difference is the large statistical significance in the full heat flux field ($\overline{v'T'}$), with the POST composite average being significantly greater than the NSW composite average for the entire composite time period, and the PRE composite average be-

ing significantly greater from day -20–+4. The climatological component ($\overline{v'_C T'_C}$) is also significantly greater in both PRE and POST composite averages when compared to the NSW composite average for days -20–+24 and -20–+30 respectively.

4.2.3 Scale Decomposition

It has been established that energy propagation from the troposphere to the stratosphere is primarily in the planetary scale (e.g. Charney and Drazin (1961)). The meridional eddy heat flux was partitioned into wave components using Fourier filtering to extract both planetary scale (wavenumbers 0–3) and synoptic scale (wn. 4–8) contributions. Figure 4.12 shows this for the group average, but only the same scale interaction between v' and T' (e.g. $v'^P T'^P$), as the opposing scale interaction terms (not shown) were several orders of magnitude smaller. As expected, the planetary scale heat fluxes in the of the full field are much larger than those on the synoptic scale. The planetary scale full heat flux also has much the same pattern as the non-partitioned full heat flux, with the PRE composite having a narrow peak before onset, and the POST composite featuring a broader peak near and after onset, with both being significantly larger in magnitude than the NSW composite. Much of this difference appears to come from the climatology, as it is significantly greater in both PRE and POST composite averages when compared with the NSW composite average for nearly the entire composite time period.

In the synoptic scale field, nearly all of the difference comes from the anomaly,

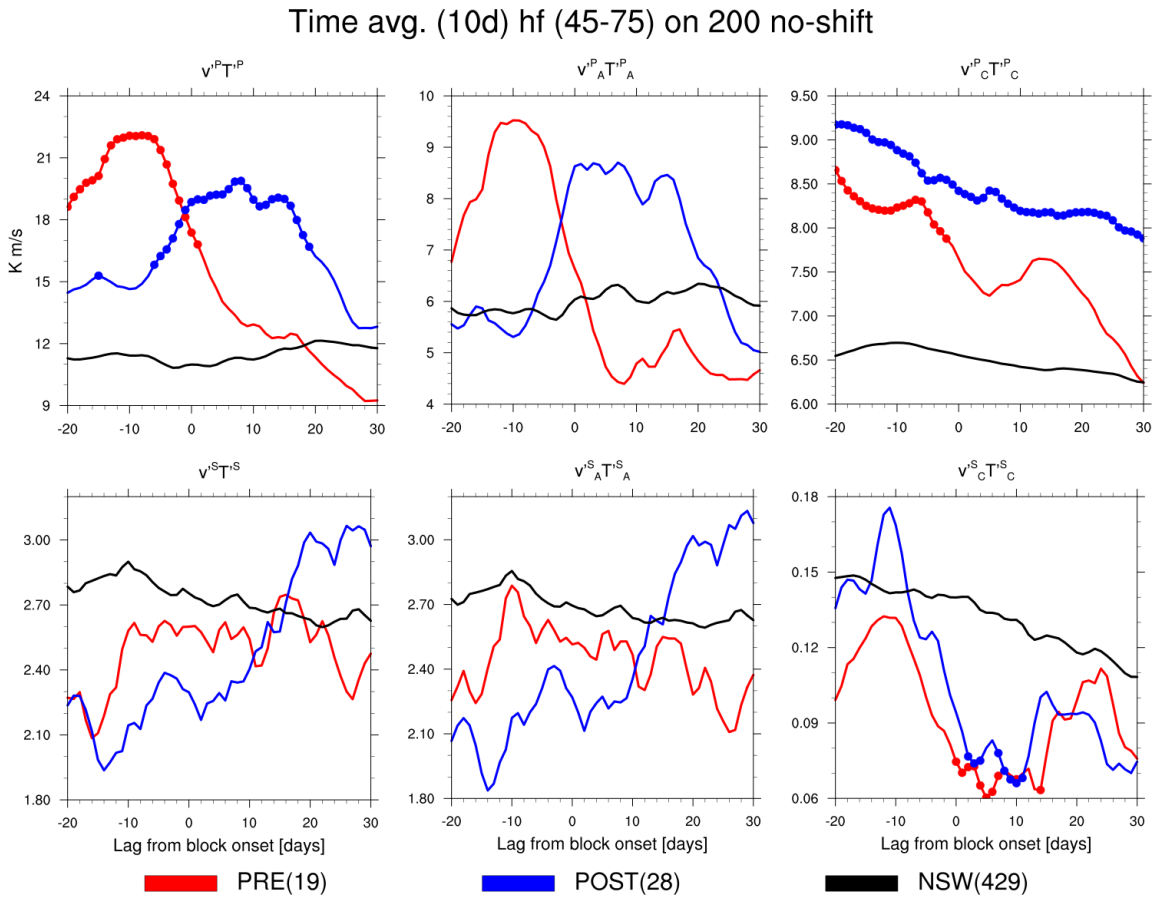

Figure 4.12: Ten day averaged meridional heat flux, scale decomposition. Superscript "P" is planetary wave component, superscript "S" is synoptic wave component. Subscripts and colors as in figure 4.6.

as expected. Unexpectedly, the NSW composite average is larger than both PRE and POST composite averages during the blocking event. The POST average does become larger near day +15, though none of these differences are statistically significant. It can be seen from figure 4.13 that the results of a different spectral filtering method yield similar results. All three composite averages have similar magnitudes in all components though Fourier filtered planetary wave full heat

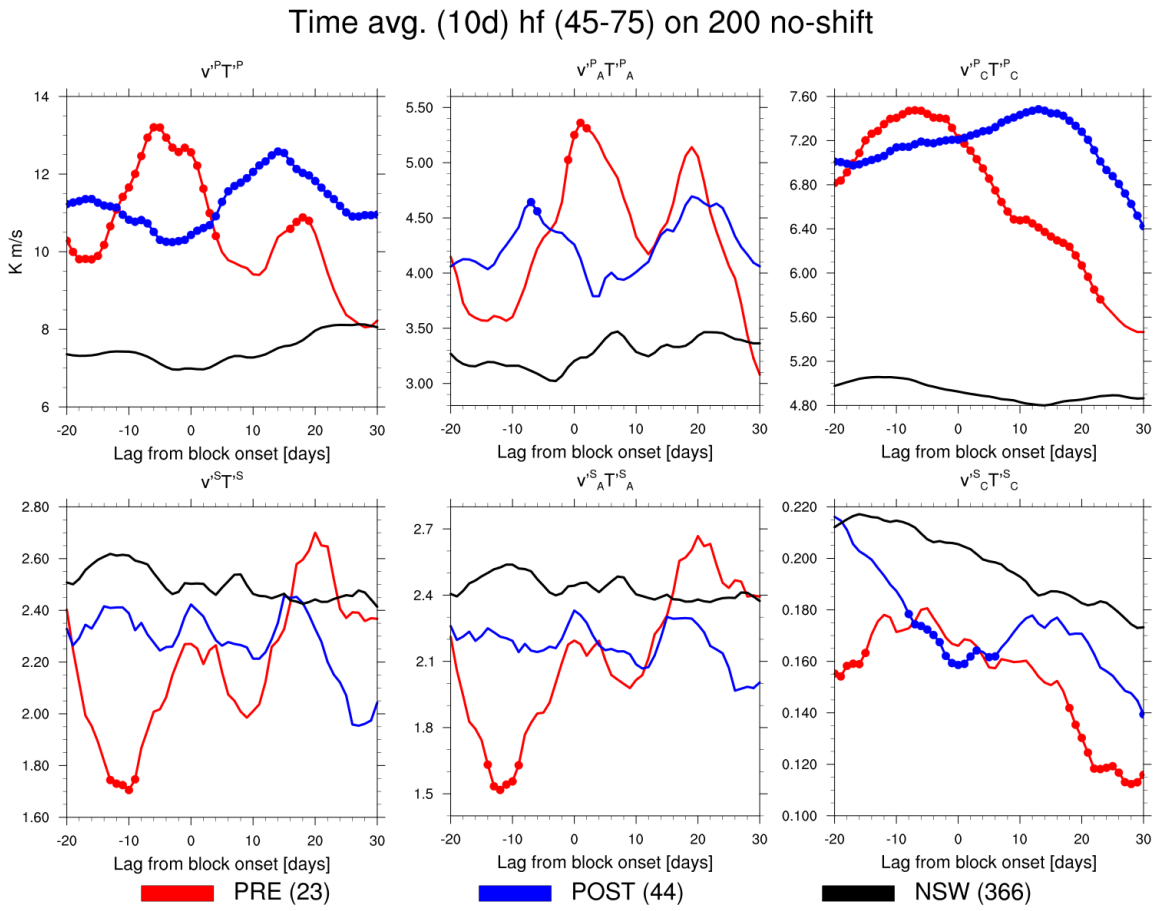

Figure 4.13: As in figure 4.12 but for Legendre transform filtered heat flux.

flux is slightly larger than its Legendre filtered counterpart. The PRE and POST composite averages in the planetary scale full heat flux field are again significantly larger than the NSW composite average, with significance extending from day -20–+4 for the PRE composite and for the entire composite time period for the POST composite.

4.3 Polar cap EPV

The time rate of change of the polar cap averaged potential vorticity, another possible distinguishing mechanism between the SSW associated blocking events and the non-associated events (NSW), has been examined by Colucci (2013) in the stratosphere for individual events. Here, the tropospheric average of this will be used, rather than the time rate of change in the stratosphere. Figure 4.14a shows that there is a dramatic decrease from days -50 – -20 in for both PRE and POST, where the NSW composite only decreases marginally, with both PRE and POST being anomalously anticyclonic in the period before onset, whereas the NSW composite is anomalously cyclonic, but very near climatology. The PV is significantly more anticyclonic (fig. 4.14b) for days -27– -15 in the PRE composite and -23 – 0 in the POST composite. After approximately day -20, in both the PRE and POST composites, the anomalous PV begins to increase, until approximately day +30, where another decrease begins. After the block onset, the anomalous PV is significantly greater in both PRE and POST composites when compared to the NSW composite.

When the polar cap PV is averaged for blocking events in each sector (figure 4.15), a similar pattern is seen with anomalously anticyclonic PV in the period before onset, after which the polar cap average PV increases to become anomalously cyclonic in both PRE and POST composite averages. There are smaller variations within each sector on the 2-5 day synoptic time scales, with the NSW composite average remaining nearly constant with a slight decrease towards and after block

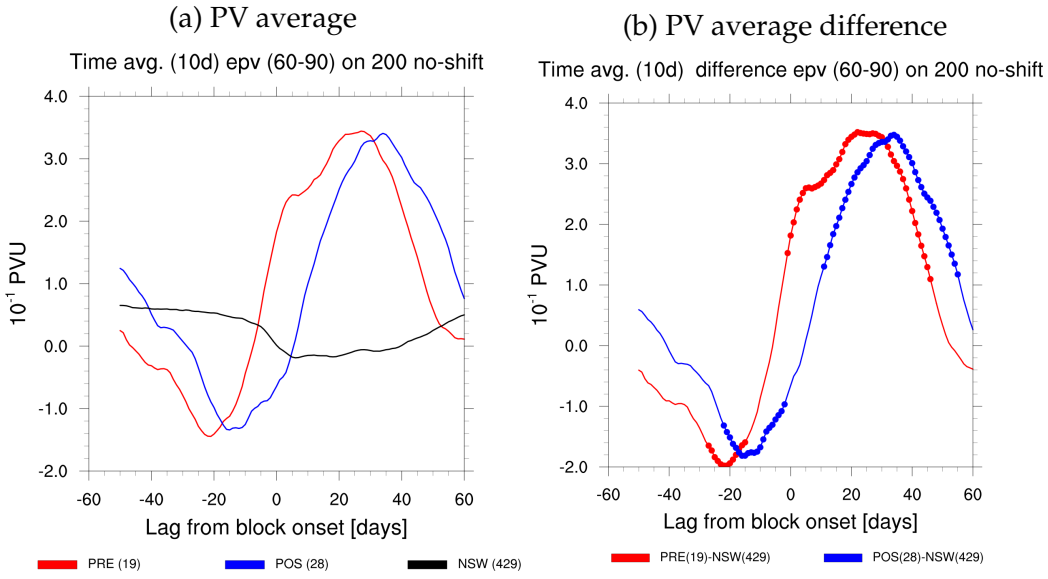

Figure 4.14: Anomaly from climatology of PV on 200 hPa for (a) composite PRE (red), POST (blue) and NSW (black), and (b) composite differences in PV anomaly between PRE and NSW (red) and POST and NSW (blue).

onset. As seen in figure 4.15b, these differences are only significant after they become more cyclonic (with the exception of one point in the Atlantic/Europe PRE composite) in both PRE and POST averages in the Atlantic/Europe composite, and the POST average in the Pacific/Asia composite. However, the Greenland POST composite average is significantly more anticyclonic before onset, up to approximately day -40, then significantly more cyclonic after onset in both the PRE and POST composite averages.

When the same procedure is applied to the minor warming associated blocking events, a somewhat different pattern is exposed. Figure 4.16 shows that, while in the major warming composites, there is a decrease in anomalous PV before on-

(a) PV average

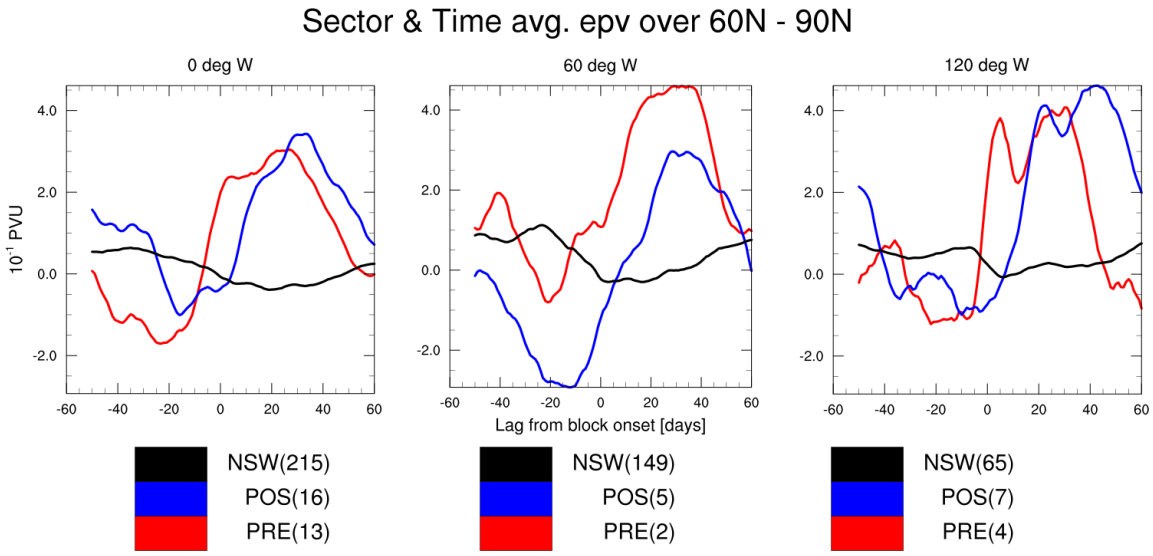

(b) PV average difference

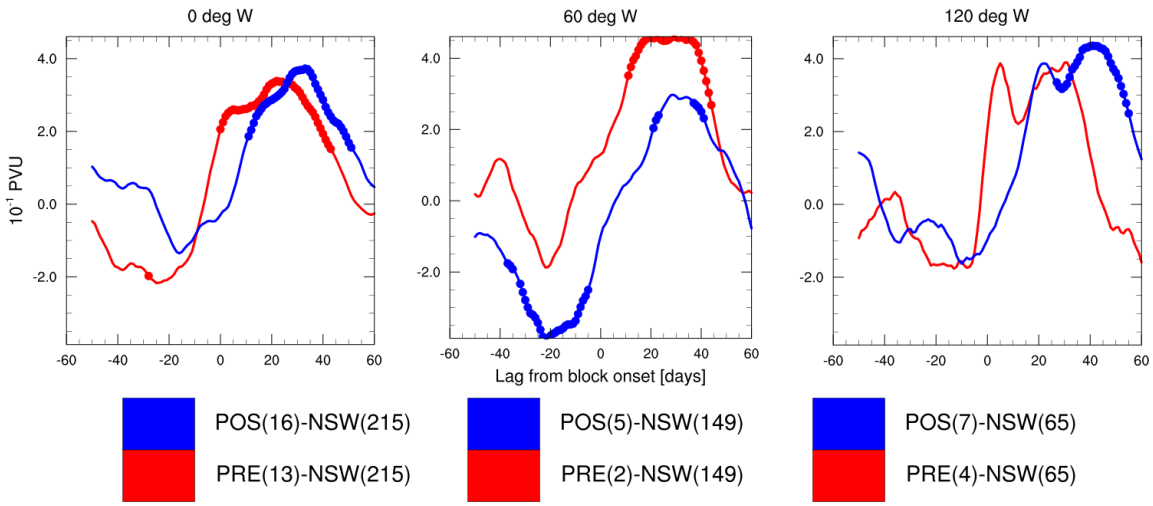

Figure 4.15: As in figure 4.14, but for sector composite averages

set, followed by a dramatic increase, in the minor warming composites, a smaller decrease before onset remains anomalously anticyclonic until approximately day +20 in the PRE composite average and day +40 in the POST composite average. In contrast to the major warming associated composites, the minor warmings associated composites only have statistically significant anticyclonic differences from the NSW composite, shown in figure 4.16b.

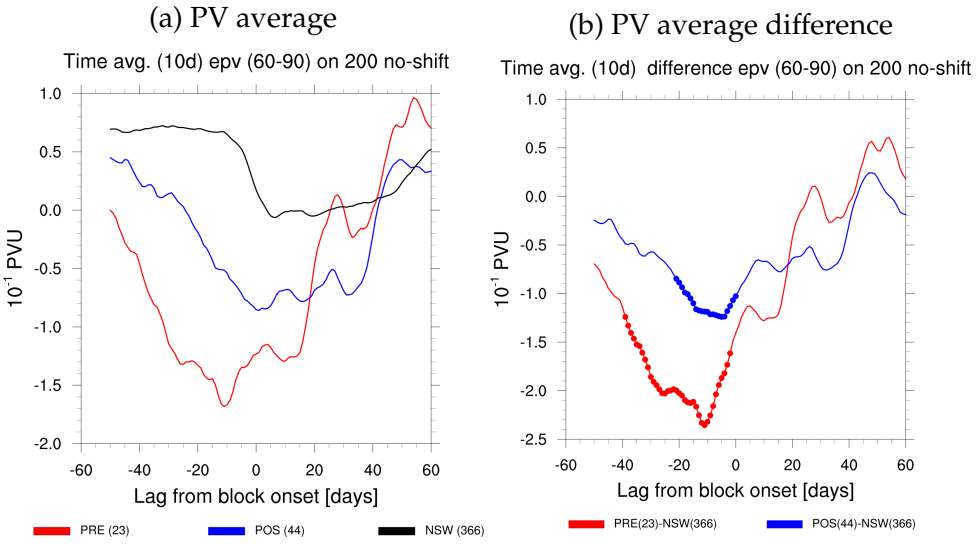

Figure 4.16: As in figure 4.14 but for events relative to minor warmings.

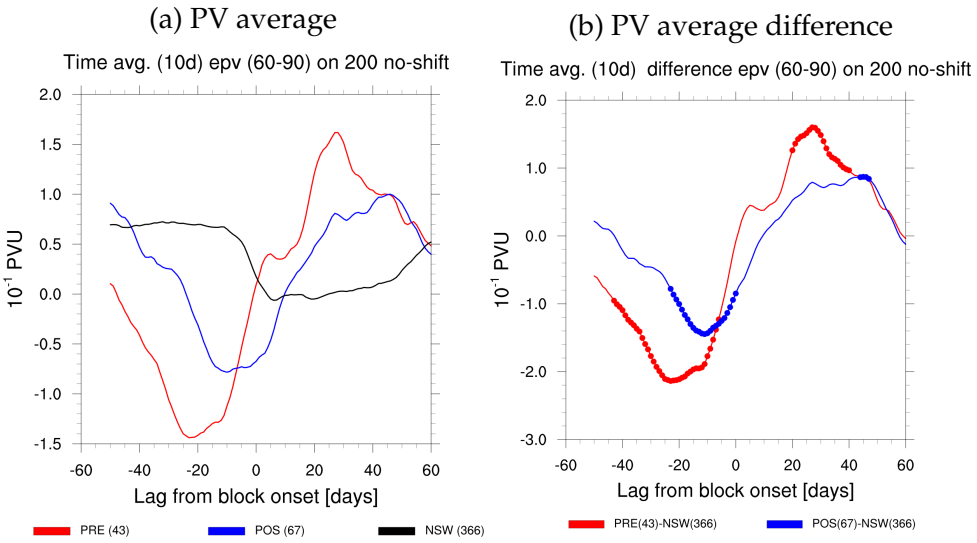

Figure 4.17: As in figure 4.14 but for events relative to all warmings.

The composite of polar cap PV for blocking events relative to all warmings is shown in figure 4.17, where a similar pattern is seen. Both PRE and POST composite averages start with large anomalous anticyclonic increases until approximately day -20 and day -15 respectively. The NSW composite also features an anticyclonic increase from days -10–+5. After onset both the PRE and POST composites transition to anomalously cyclonic polar cap average PV, which is significant (fig. 4.17b) for days +20–+40 and +45–+50 respectively.

4.4 Summary

In this chapter, a detailed account of differences between blocking events associated with SSW events and blocking events lacking an associated SSW event was presented. Statistically significant differences were found in the stratospheric height field (Aleutian high) and the zonal mean zonal wind field in the stratosphere, though these are indicators of SSWs rather than predictive. It was also found that time averaged tropospheric meridional eddy heat flux is significantly greater during blocking events associated with SSW events than in blocking events not associated with SSW events for both major and minor warmings. When this heat flux is separated into sector averages, there are small time windows of significant differences between groups, but a larger pattern does not emerge. The planetary scale components of this heat flux are also significantly greater during blocking events associated with SSWs when compared to those that are not, while

the synoptic scale components showed no such distinction.

The tropospheric polar-cap averaged PV was shown to be significantly more anticyclonic with a very long time lead (up to 40 days) in advance of block onset and significantly more cyclonic after block onset. When this was examined in relation to where the blocking event occurred, the differences were also significant after onset, though there was less significance before onset. These calculations were repeated for blocking events associated with minor warmings with similar results.

CHAPTER 5

COMPOSITES: INTERFERENCE GROUPING

5.1 Heat flux

To better understand the role of blocking that occurs in climatologicaly favorable conditions when compared to unfavorable conditions, blocking events were grouped by whether the relative vorticity in the blocking region was constructively or destructively interfering with the climatological relative vorticity, then composites were generated as before, with an interference group rather than a sector. Figure 5.1 illustrates that slight differences exist in the heat flux fields of these events, though the number of events in each group are not dissimilar.

Firstly, examining the full heat flux field, the familiar pattern is apparent, with the PRE composite average peaking before onset, the POST average just before and after onset, while the NSW average lacks a peak. Though here, the PRE and POST averages for destructive interference blocking events peak earlier than their constructive interference counterparts by approximately 5 and 8 days respectively. In the PRE composite average, this appears to come from both the anomalous advection of climatological temperature ($\overline{v'_A T'_C}$) and the climatological advection of anomalous temperature ($\overline{v'_C T'_A}$) as both are significantly greater than in the NSW composite average before the onset of blocking. In the POST composite average the this is aided by the anomaly ($\overline{v'_A T'_A}$), though not statistically significant, in addition to the significant anomalous advection of climatological temperature. Also in

the POST average, the climatological advection of anomalous temperature ($\overline{v'_C T'_A}$) partially accounts for the longer lasting heat fluxes.

As one might expect, the climatology ($\overline{v'_C T'_C}$) plays a greater role in the de-

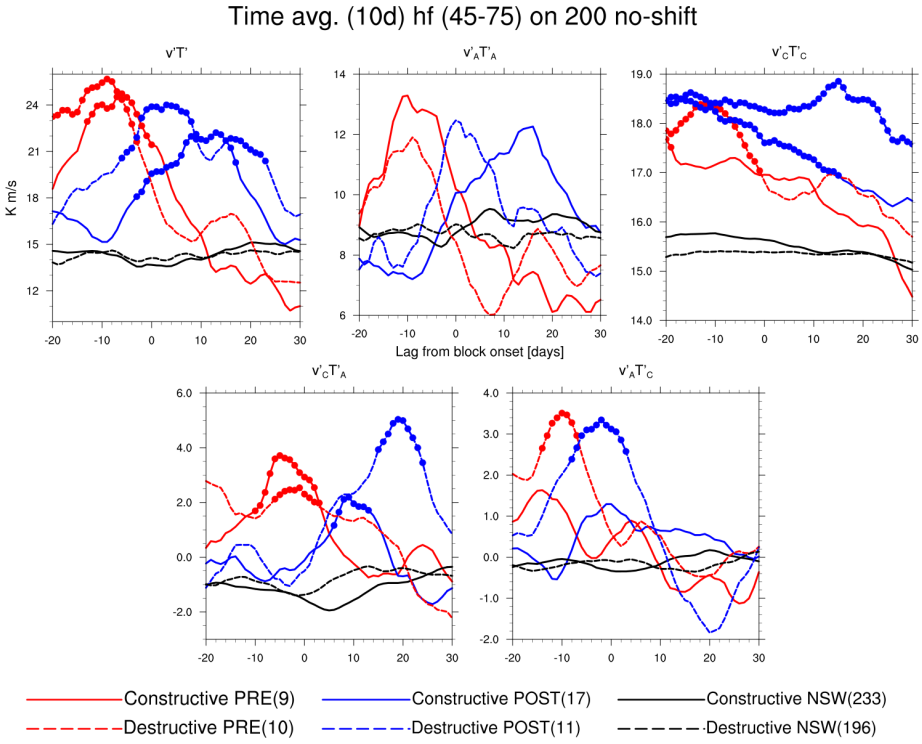

Figure 5.1: Zonal average, ten day average composite heat flux for interference grouping. Red lines for PRE composite, blue indicates POST, black for NSW, while solid lines indicate constructive interference, dashed indicates destructive. Subscript "C" indicates climatology component, subscript "A" indicates anomaly from climatology component.

structive interference blocking events, especially in the POST composite average, and there is very little difference in the NSW composite average.

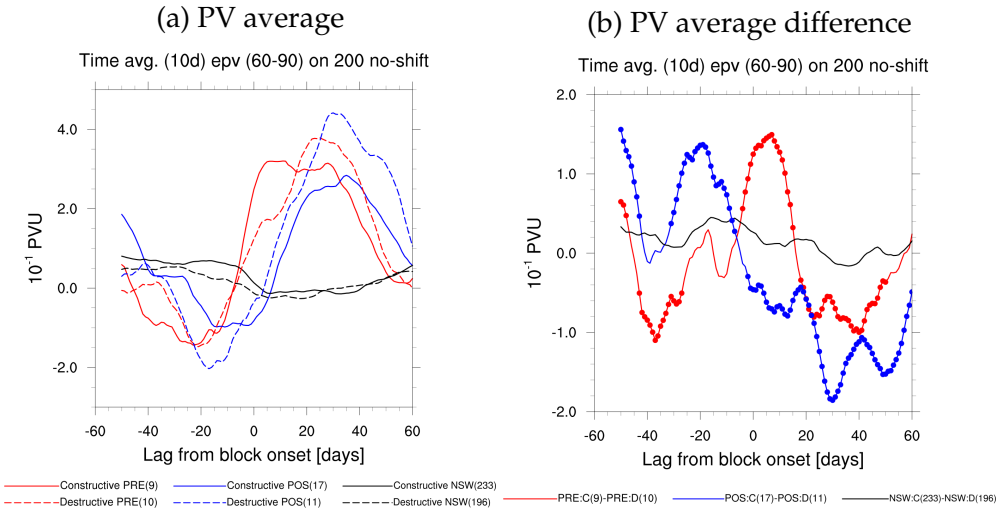

Figure 5.2: (a) Polar cap and time averaged PV at 200 hPa. Colors indicate temporal group (red:PRE, blue:POST, black:NSW), and dash pattern indicates interference type (solid:constructive, dashed:destructive). (b) As in (a) but for difference between interference type for each group is shown with markers indicating statistical significance to $\alpha = 0.01$.

5.2 EPV

The polar cap PV composite average was also investigated for these composites, and the results presented in figure 5.2a. The familiar pattern of polar cap PV anomaly presents again, an anticyclonic increase before onset, and cyclonic increase after onset. The differences of PRE and POST from NSW composite averages (not shown) are also statistically significant, as before. Shown in figure 5.2b though, are the differences between constructive and destructive events within each temporal group, which are also statistically significant.

The constructive interference PRE composite average is significantly more cyclonic in a short period near day -50, then significantly more anticyclonic from approximately day -45 – -25. It then becomes significantly more cyclonic just before and after onset, from approximately day -5 – +15, after which it becomes significantly more anticyclonic again from days +20 – +50. This can be contrasted to the POST composite average, which is significantly more cyclonic early (days -50 – -45, -30 – -5), and significantly more anticyclonic late (days 0–+60). The NSW composite average is not significantly different between constructive and destructive interference events.

5.3 Summary

In this chapter, blocking events were grouped by their interaction with climatology rather than location. Statistically significant differences were again found between the meridional eddy heat fluxes during blocking events associated with SSW events from blocking events that were not, though significant differences were not seen between the constructive and destructive interference groups. The polar-cap averaged PV, however, did exhibit significant differences. In the PRE composite average, the constructive interference blocking events were significantly more anticyclonic both before and after onset, while nearest onset, they featured significantly more cyclonic PV. In the POST composite average, the constructive interference blocking events had significantly greater cyclonic PV in ad-

vance of block onset, transitioning to significantly greater anticyclonic PV after onset.

CHAPTER 6

COMPOSITES: GROUPED BY SECTOR MERRA

As there are questions to the accuracy of the stratospheric representation in the NCEP/NCAR Reanalysis I (Trenberth and Stepaniak, 2002), a second dataset was needed to bolster the results already presented. As stated above, NASA's MERRA was chosen for its better stratospheric representation. Shown here are the results from the composites of blocking events relative to both major and minor warmings, as the MERRA data spans 1979-present, though blocking events from 1980-2010 were used to compare with the NCEP/NCAR Reanalysis directly. There are fewer warming events to examine, thus using both major and minor warmings presents the best opportunity for statistical significance. This is the same rationale for presenting the meridional eddy heat flux and polar cap PV average results, as those have given the most significant results in the NCEP/NCAR Reanalysis data.

6.1 Heat flux

The meridional eddy heat flux, shown here in figure 6.1, has the familiar pattern from the NCEP/NCAR Reanalysis present in the full field. The PRE composite average peaks before onset from approximately day -10–0 and is significantly greater than the NSW composite from day -30–+4, with the POST composite average peaking from approximately day 0–+10 and being significantly greater from

day -20–+24. The NSW composite average again does not have a peak, and remains very close to climatology. The full field matches well between NCEP and MERRA, while the difference is the dramatic dip in the PRE composite average after onset, which then recovers shortly after, though this is not statistically significant.

In the NCEP/NCAR dataset, the heat flux from sectors external to blocking appears important in some cases; thus it is also examined here for MERRA data. In the Atlantic/Europe composite, there is a large contribution from external sectors, especially in the PRE composite average (fig.6.2), with the downstream sector being significantly greater near onset in both PRE and POST composite averages when compared to the NSW composite average in the downstream sector. This appears to be the result of the climatological contribution in the PRE composite average, as it is significantly greater than its NSW counterpart in the downstream sector, which is different from the NCEP results of the same time period (fig 6.3), which appear similar to the larger time period of NCEP reanalysis.

With only two events, in each PRE and POST in the Greenland composite averages, results are not as conclusive, with only a single point of significance in the full field near onset, with the POST composite average being significantly less in the downstream sector than in the NSW composite downstream sector.

The Pacific/Asia composites also appear dissimilar in the MERRA results when compared to the NCEP results on the same time period, with the blocking sector having a strong contribution to both PRE and POST averages, with statistical significance near block onset, though a similarity is that both PRE and POST

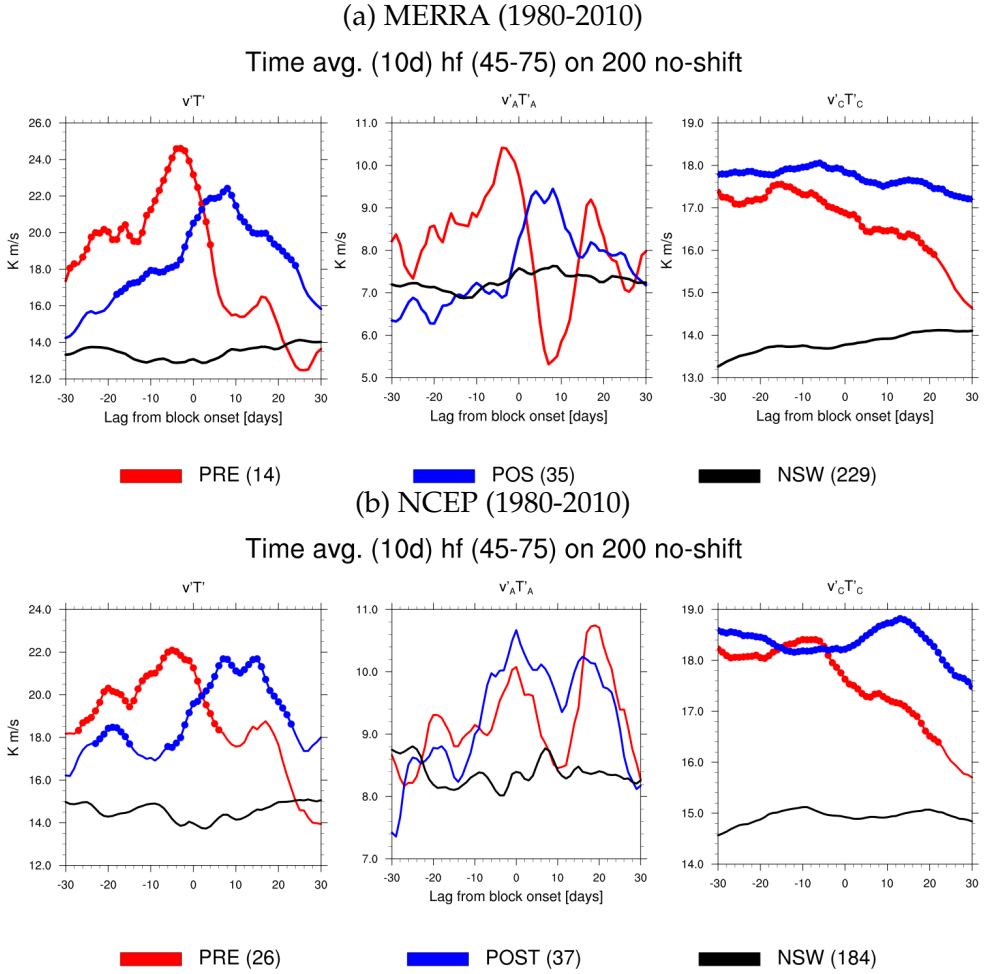

Figure 6.1: As in figure 4.6, but for MERRA analyzed events (top) and NCEP analyzed events (bottom) from 1989-2010, relative to all stratospheric warmings.

upstream climatological composite averages are statistically significant in NCEP as well as MERRA for nearly the entire composite time period.

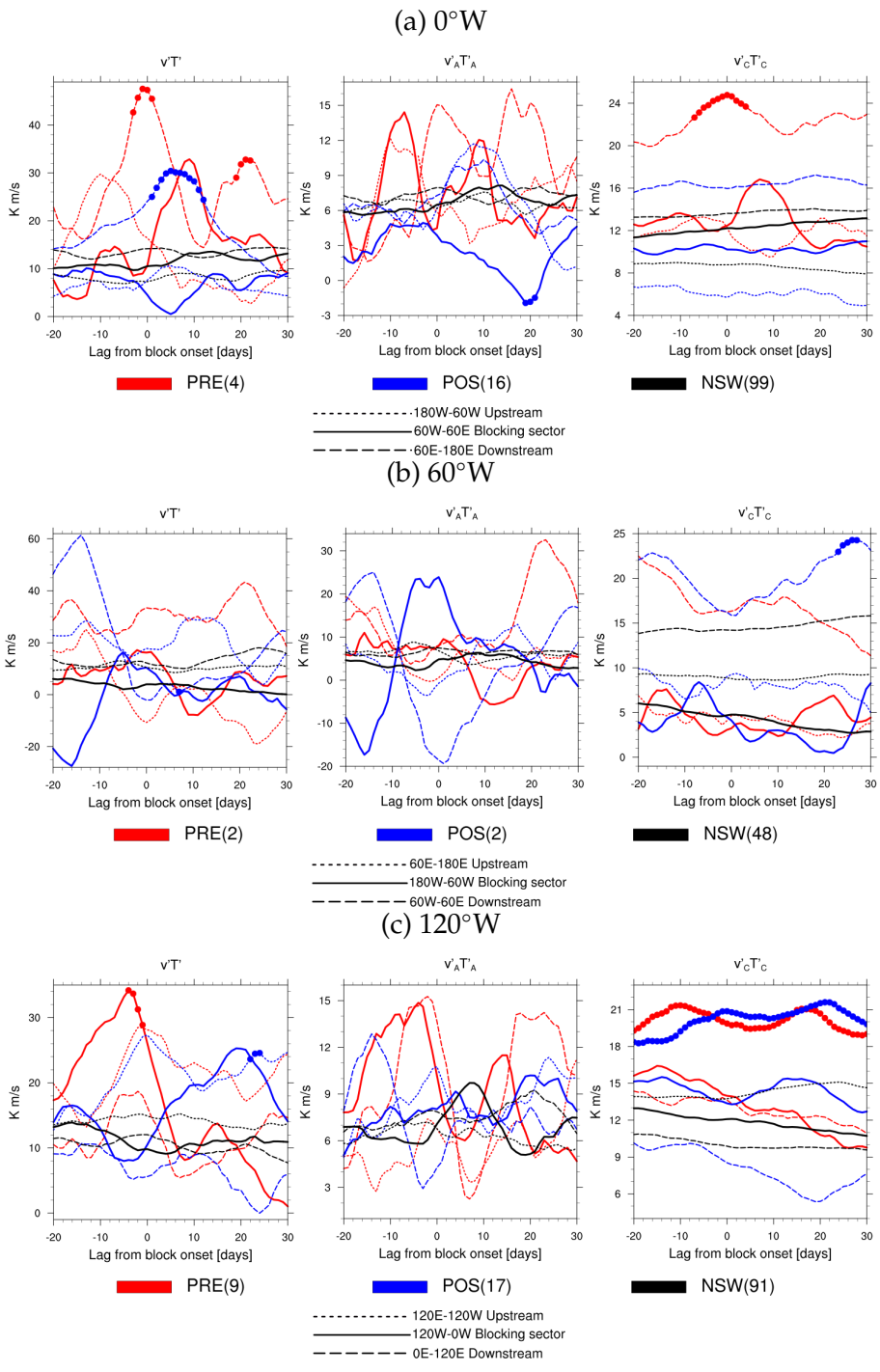

Figure 6.2: As in figure 4.8, but for events in MERRA relative to all warmings.

(a) 0°W

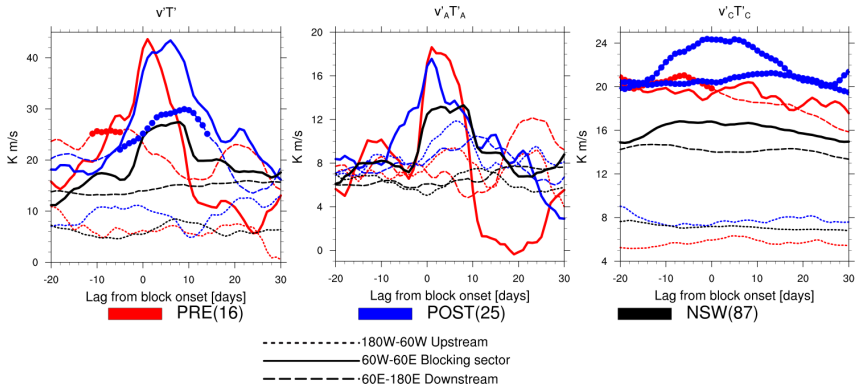

(b) 60°W

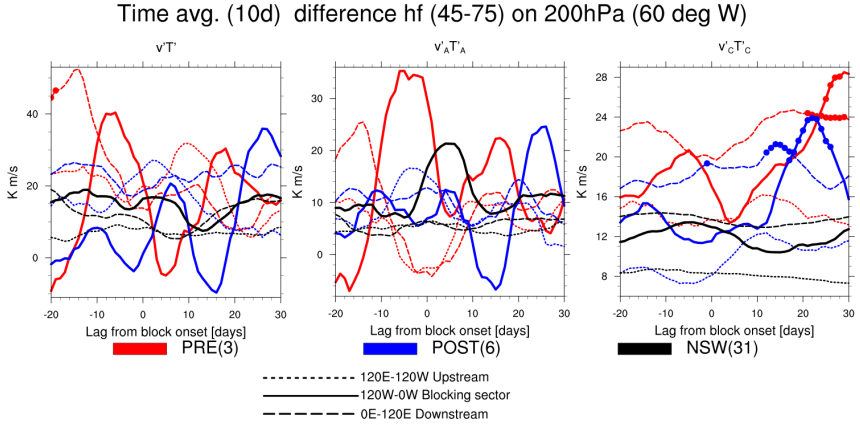

(c) 120°W

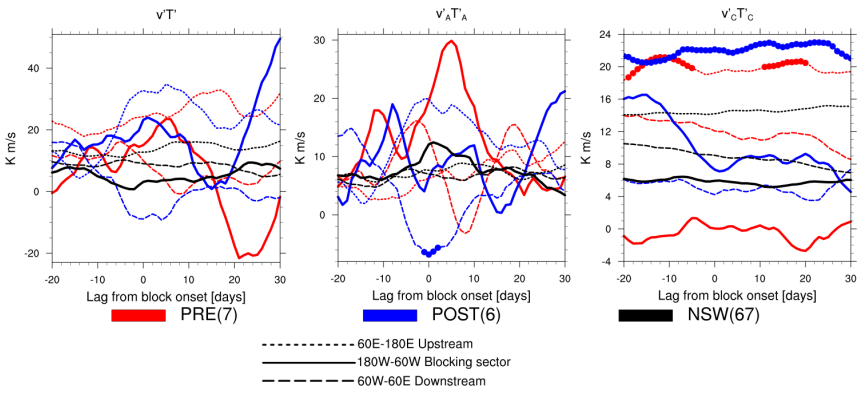

Figure 6.3: As in figure 4.8, but for events in NCEP relative to all warmings during 1980-2010.

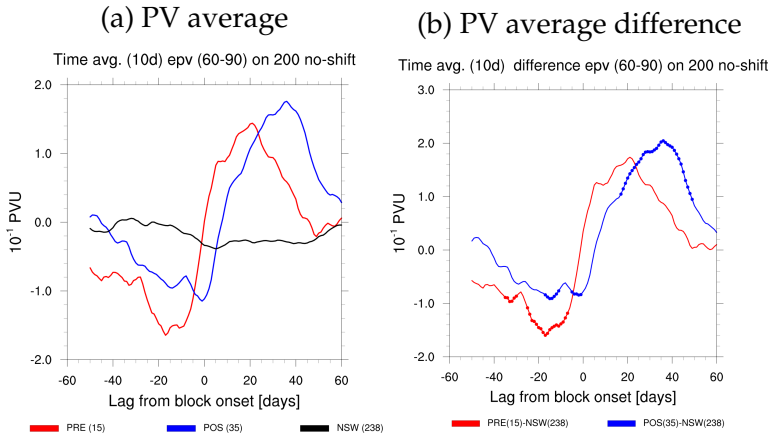

Figure 6.4: As in figure 4.14 but for MERRA events relative to all warmings, and significance is shown to $\alpha = 0.1$.

6.2 EPV

The familiar pattern in tropospheric polar cap averaged PV is again seen in the MERRA events relative to all warmings, shown in figure 6.4. There is anomalous anticyclonic PV in the lead up to onset, from around day -50, then near onset there is an increase in cyclonic PV leading to anomalously cyclonic PV at or just after onset in both PRE and POST composite averages, with the PRE composite average transitioning approximately 5 days before the POST average.

The differences in these fields (figure 6.4b) are not as statistically significant as in the NCEP/NCAR events. This is potentially caused by the lower number of events as the deviations are of similar magnitude. The PRE composite average is

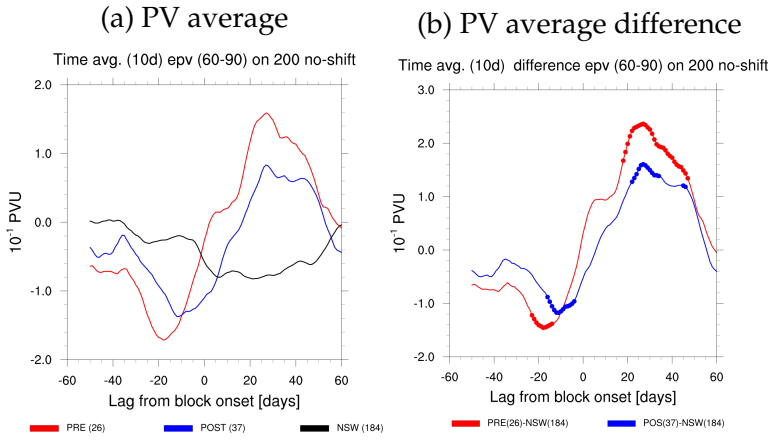

Figure 6.5: As in figure 4.14 but for NCEP events relative to all warmings during 1980-2010 and significance is shown to $\alpha = 0.1$.

significantly more anticyclonic for approximately days -40 – -5, while the POST composite average is for days -20 – 0. The PRE composite average does not have significantly greater cyclonic PV after onset as it did in the NCEP/NCAR events, but the POST composite average features significant cyclonic anomalies from day +15–+45. These results compare very well with the results from the same period of time with NCEP analyzed events (fig. 6.5), though the NCEP results feature shorter periods of statistical significance before onset, but cyclonic significance in both PRE and POST composites rather than just POST as in MERRA.

6.3 Summary

As questions have arisen to the accuracy of the NCEP/NCAR Reanalysis dataset, especially its stratospheric representation, a second dataset was used for comparison. Similar results were seen in both overall average meridional eddy heat flux, polar-cap PV, especially when compared with identical time periods in both data sets. The two data sets diverge on the sector average heat fluxes, though neither data set has large statistical significance except in climatological differences between blocking events associated with SSW events from those that are not. Though there are fewer events, long-time lead statistical significance is still seen in both polar-cap PV and zonal averaged meridional eddy heat flux.

CHAPTER 7

FORECASTING SSW EVENTS

The essence of science is using data gathered to make predictions, thus the trends observed here were used as single measure forecast methods to predict SSW events, major or minor. The skill of the forecast was assessed using the Gilbert Skill Score (Gilbert, 1884), which takes into account the prediction rate, the false alarm rate, as well as a "random chance" forecast. This is shown in equation 7.1 where a is the number correctly forecasted, a_R is a "random chance" correct forecast, here designated to be the long term climatological probability of SSW occurrence within 60 days of any wintertime day, b is the number of false alarm forecasts, and c is the number of warmings that were not successfully predicted. Here a successful forecast is designated as one that occurs less than 60 days and more than a threshold of days before an SSW key date, such that the entire polar-cap PV anomaly or zonal average heat flux event takes place before the SSW event. Positive values of GSS mean that the predictor is better than random chance, while negative values indicate the opposite.

$$GSS = \frac{a - a_R}{a - a_R + b + c} \tag{7.1}$$

The polar-cap averaged PV was previously shown to be significantly anticyclonic up to 40 days in advance of block onset, thus shows potential as a long-term forecast metric. Figure 7.1 shows the skill score of the polar-cap averaged PV climatological anomaly at 200 hPa as a function of various thresholds. The skill is

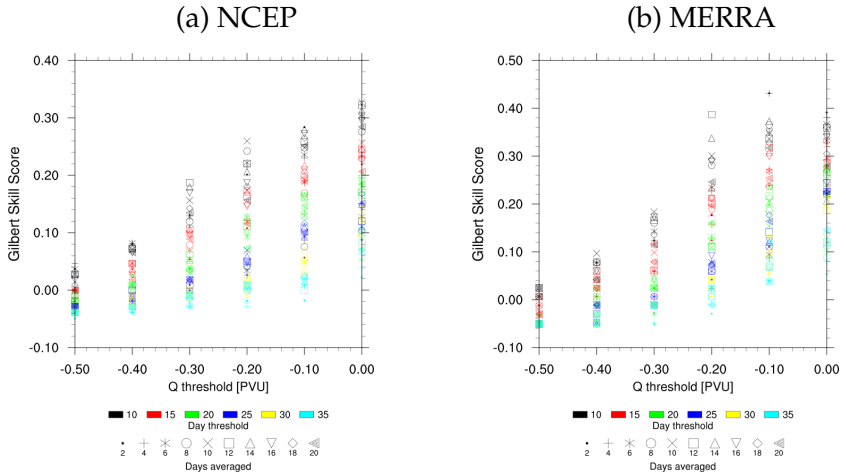

Figure 7.1: Gilbert skill score by thresholds. Marker shape indicates number of days polar-cap PV is averaged, maker color indicates threshold of number of consecutive days PV anomaly must be below the PV threshold shown on the x-axis.

maximized at 0.33 in the NCEP data set (fig. 7.1a) when using 10 day averaged polar cap PV below 0 PVU for 10 or more days, and at .43 in the MERRA data set when using either 2 or 4 day averaged polar cap PV below -0.1 PVU for 10 or more days.

The same technique was used with the zonally averaged meridional eddy heat flux (45°– 75°N) at 200 hPa, and the results are shown in figure 7.2. The skill here is better than using the polar-cap averaged PV for each data set, with the maximum in NCEP of 0.46 for 14 day averaged heat flux greater than 17 K m/s for 2 or more days, and in MERRA of 0.76 for 10 day averaged heat flux greater than 18 K m/s for 2 or more days. These scores indicate that while both tropospheric meridional eddy heat flux and polar-cap PV are better forecast metrics than the climatological probability, there is room for improvement.

(a) NCEP (b) MERRA

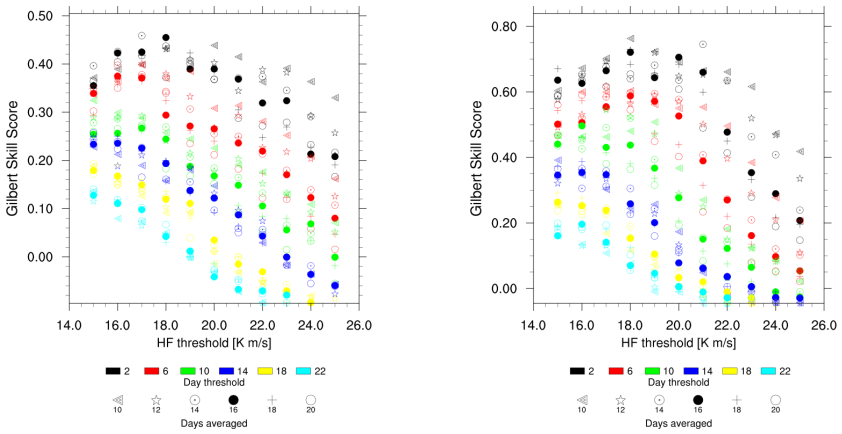

Figure 7.2: As in figure 7.1 but for heat flux above the x-axis threshold

7.1 Summary

As both polar-cap averaged PV anomaly from climatology and zonally averaged meridional eddy heat flux featured statistical significance at long time leads from the onset of blocking events, their viability as predictors of SSW events was tested in this chapter. It was found that both polar-cap averaged PV and zonal average heat flux have some skill over climatology. The zonal average heat flux was found to have the best skill regardless of data set, and both predictors had better skill in MERRA than in the NCEP reanalysis.

CHAPTER 8

CONCLUSIONS

Presented here are several methods for distinguishing blocking events associated with sudden stratospheric warmings from blocking events not associated with SSWs. The first of which was that the duration of blocking events associated with major SSWs were longer than non-associated events. This was significant for events in the Atlantic/Europe and Pacific/Asia sectors that were followed by SSWs in the NCEP data and significantly longer for blocking events followed by any type of warming in the MERRA data.

Secondly, the composite geopotential height field, which features large anticyclones for all composites (except during Greenland blocking events) in the wave breaking identified region with differentiation from the NSW composite only appearing due to the large number of events smoothing the field, thus the geopotential height field cannot be used to differentiate blocking events associated with SSWs from those that are not. Though in the stratosphere, a closed anticyclone at 10 hPa known as the Aleutian high is present in SSW associated blocking events, while absent in the NSW events.

The evolution of the PV field on 200 hPa was also presented. With only small areas of statistical significance present, this is also not a distinguishing feature between SSW associated blocking events from blocking events that are not.

The connection between the stratosphere and troposphere was apparent in the SSW associated composite zonal mean zonal wind fields. With PRE events

in general, the stratosphere led decreases in the troposphere, while in the POST events, the troposphere led the stratosphere. This connection was absent in the Atlantic/Europe and Pacific/Asia composite U-wind field in NSW events, but there appeared to be a zonal mean zonal wind precursor in the stratosphere during the Greenland NSW events that was 30 days before block onset. This is interesting, as the signature could potentially be an SSW, as 30 days prior to onset is outside the 10 day time frame set here. Upon further investigation, it is not from SSW events major or minor, only a weakening of the polar stratospheric vortex that does not meet either condition.

Long duration anomalous meridional eddy heat flux has been found to be associated with SSW events, major and minor, thus it is expected that blocking events associated with SSW events will have increased heat flux, and this was found to be the case. In major and minor warming events, the heat flux was enhanced before block onset in PRE events, and at or after onset in POST events, with magnitude coming from climatological values, and oscillation from anomalous values. The non-SSW blocking events lacked this signature.

When the heat flux was separated into sector averages, the blocking sector was found to contribute, though it was at times outweighed by external contributions, especially in the Greenland and Atlantic/Europe composites. Climatology also played an important role, with much of the sector average differences resulting from differences in climatological patterns, meaning that when in the season blocking events occur is important to stratospheric influence. Though differences here are not statistically significant. When separating the heat flux averages into

planetary and synoptic wave components, it was seen that the contribution to the total heat flux was mainly on the planetary scale, and larger in both SSW associated composite averages. On the synoptic scale, there was enhanced activity in the NSW associated composites, though the differences were not significant, meaning that the synoptic scale heat fluxes have little influence on whether a blocking event is associated with a stratospheric warming event.

Examining the tropospheric polar cap PV also presented a stark difference between SSW associated events and non-associated events, with anticyclonic anomalies before onset that transition through onset to become cyclonic anomalies. In several of the composites these differences were statistically significant for nearly two months before block onset, which generated the idea of using this as an indicator for the prediction of a stratospheric warming, major or minor, with some success. This was also tested using zonally averaged meridional heat flux as an indicator, with improved forecast ability.

CHAPTER 9

DISCUSSION

The particular problem of the association of sudden stratospheric warming events with tropospheric blocking events is the small sample size of sudden stratospheric warming events, especially major events, though that is part of what makes these events scientifically interesting. Previous authors have focused on the composite behavior of SSW events both major and minor, as well as composite blocking events. This study has specifically sought a distinction between blocking events that occur near in time to SSW events and blocking events not associated with SSW events, as there are many more blocking events in this latter category.

Three statistically significant indicators have been found: the Aleutian high (present in SSW associated blocking events, not in non-associated events), the time averaged zonally averaged tropospheric meridional eddy heat flux (much larger in SSW associated blocking events), and time averaged polar-cap tropospheric PV climatological anomaly, which is significantly more anticyclonic up to 50 days before blocking and significantly more cyclonic after onset in the blocking events associated with SSW events.

It is speculated here that the pattern seen in the polar-cap averaged tropospheric PV anomaly is due to a bi-directional association between the stratosphere and troposphere. The long time lead in the anticyclonic anomaly in the troposphere may be a result of stratospheric forcing on tropospheric conditions, with the increase after block onset being a response to this. Further investigation is

needed in this area, as long time leads are useful in generating meaningful long-term forecasts as well as assessing climate variability. This may be accomplished by a series of modeling experiments, whereby stratospheric conditions are varied with a fixed troposphere, and tropospheric conditions are varied with a fixed stratosphere to generate correlations between upward and downward fluxes of energy between the two layers.

BIBLIOGRAPHY

Anderson, C. J. and R. W. Arritt, 2001: Representation of summertime low-level jets in the central united states by the ncep–ncar reanalysis. *Journal of Climate*, **14 (2)**, 234–247.

Baldwin, M. P. and T. J. Dunkerton, 2001: Stratospheric harbingers of anomalous weather regimes. *Science*, **294 (5542)**, 581–584.

Baldwin, M. P., D. B. Stephenson, D. W. J. Thompson, T. J. Dunkerton, A. J. Charlton, and A. O'Neill, 2003: Stratospheric memory and skill of extended-range weather forecasts. *Science*, **301 (5633)**, 636–640.

Bao, X. and F. Zhang, 2012: Evaluation of ncep–cfsr, ncep–ncar, era-interim, and era-40 reanalysis datasets against independent sounding observations over the tibetan plateau. *Journal of Climate*, **26 (1)**, 206–214.

Bosilovich, M. G., F. R. Robertson, and J. Chen, 2011: Global energy and water budgets in merra. *Journal of Climate*, **24 (22)**, 5721–5739.

Brunke, M. A., Z. Wang, X. Zeng, M. Bosilovich, and C.-L. Shie, 2011: An assessment of the uncertainties in ocean surface turbulent fluxes in 11 reanalysis, satellite-derived, and combined global datasets. *Journal of Climate*, **24 (21)**, 5469–5493.

Carrera, M. L., R. W. Higgins, and V. E. Kousky, 2004: Downstream weather impacts associated with atmospheric blocking over the northeast pacific. *J. Clim.*, **17 (24)**, 4823–4839.

Charlton, A. and L. Polvani, 2007: A new look at stratospheric sudden warmings. part i: Climatology and modeling benchmarks. *J. Clim.*, **20**, 449–469.

Charney, J. G. and P. G. Drazin, 1961: Propagation of planetary-scale disturbances from the lower into the upper atmosphere. *Journal of Geophysical Research*, **66**, 83–109.

Christiansen, B., 2001: Downward propagation of zonal mean zonal wind anomalies from the stratosphere to the troposphere: Model and reanalysis. *Journal of Geophysical Research: Atmospheres*, **106 (D21)**, 27 307–27 322.

Colucci, S. J., 2013: Diagnostic comparison of tropospheric blocking with and without stratospheric warming. *Submitted to J. Atmos. Sci.*

Eliassen, A. and E. Palm, 1961: *On the tansfer of energy in stationary mountain wave.*, Vol. 22. 1-23 pp.

Esler, J. G. and N. J. Matthewman, 2011: Stratospheric sudden warmings as self-tuning resonances. part ii: Vortex displacement events. *Journal of the Atmospheric Sciences*, **68 (11)**, 2505–2523.

García-Herrera, R. and D. Barriopedro, 2006: Northern hemisphere snow cover and atmospheric blocking variability. *Journal of Geophysical Research: Atmospheres*, **111 (D21)**.

Garfinkel, C. I., D. L. Hartmann, and F. Sassi, 2010: Tropospheric precursors of anomalous northern hemisphere stratospheric polar vortices. *J. Clim.*, **23**, 3282–3299.

Gilbert, G. K., 1884: Finley's tornado predictions. *Amer. Meteor. J.*, **1**, 166–172.

Harvey, V. L. and M. H. Hitchman, 1996: A climatology of the aleutian high. *Journal of the Atmospheric Sciences*, **53 (14)**, 2088–2102.

Kalnay, E., et al., 1996: The NCEP/NCAR 40-year reanalysis project. *Bull. Amer. Meteor. Soc.*, **77**, 437–470.

Koermer, J. P., A. Kasahara, and S. K. Kao, 1983: Numerical studies of major and minor stratospheric warmings caused by orographic forcing. *Journal of the Atmospheric Sciences*, **40 (6)**, 1552–1570.

L'Ecuyer, P. and S. Côté, 1991: Implementing a random number package with splitting facilities. *ACM Transactions on Mathematical Software*, **17:1**, 98–111.

Martius, O., L. M. Polvani, and H. C. Davies, 2009: Blocking pre-cursors to stratospheric sudden warming events. *Geophys. Res. Lett.*, **36**.

Matthewman, N. J. and J. G. Esler, 2011: Stratospheric sudden warmings as self-tuning resonances. part i: Vortex splitting events. *Journal of the Atmospheric Sciences*, **68 (11)**, 2481–2504.

Mitchell, D. M., A. J. Charlton-Perez, and L. J. Gray, 2010: Characterizing the variability and extremes of the stratospheric polar vortices using 2d moment analysis. *Journal of the Atmospheric Sciences*, **68 (6)**, 1194–1213.

Mitchell, D. M., L. J. Gray, J. Anstey, M. P. Baldwin, and A. J. Charlton-Perez, 2012: The influence of stratospheric vortex displacements and splits on surface climate. *Journal of Climate*, **26 (8)**, 2668–2682.

Namias, J., 1947: Characteristics of the general circulation over the northern hemisphere during the abnormal winter 1946–47. *Monthly Weather Review*, **75 (8)**, 145–152.

Newman, P. A. and E. R. Nash, 2001: Quantifying the wave driving of the stratosphere. *J. Geophys. Res.*, **105**, 12 485–12 497.

Nishii, K., H. Nakamura, and Y. J. Orsolini, 2011: Geographical dependence observed in blocking high influence on the stratospheric variability through enhancement and suppression of upward planetary-wave propagation. *J. Clim*, **24**, 6408–6423.

Pelly, J. and B. Hoskins, 2003: A new perspective on blocking. *J. Atmos. Sci.*, **60**, 743–755.

Quiroz, R. S., 1986: The association of stratospheric warmings with tropospheric blocking. *J. Geophys. Res.*, **91**, 5277–5285.

Rex, D. F., 1950: Blocking action in the middle troposphere and its effect upon regional climate. *Tellus*, **2 (3)**, 196–211.

Rienecker, M. M., et al., 2011: MERRA: NASA's modern-era retrospective analysis for research and applications. *Journal of Climate*, **24 (14)**, 3624–3648.

Rossby, C.-G., 1945: On the propagation of frequencies and energy in certain types of oceanic and atmospheric waves. *Journal of Meteorology*, **2 (4)**, 187–204.

Sardeshmukh, P. D. and B. I. Hoskins, 1984: Spatial smoothing on the sphere. *Monthly Weather Review*, **112 (12)**, 2524–2529.

Scinocca, J. F. and P. H. Haynes, 1998: Dynamical forcing of stratospheric planetary waves by tropospheric baroclinic eddies. *J. Atmos. Sci.*, **55 (14)**, 2361–2392.

Seviour, W. J. M., D. M. Mitchell, and L. J. Gray, 2013: A practical method to identify displaced and split stratospheric polar vortex events. *Geophysical Research Letters*, **40 (19)**, 5268–5273.

Sjoberg, J. P. and T. Birner, 2012: Transient tropospheric forcing of sudden stratospheric warmings. *J. Atmos. Sci.*, **69**, 3420–3432.

Smith, S. R., D. M. Legler, and K. V. Verzone, 2001: Quantifying uncertainties in ncep reanalyses using high-quality research vessel observations. *Journal of Climate*, **14 (20)**, 4062–4072.

Taguchi, M., 2008: Is there a statistical connection between stratospheric sudden warming and tropospheric blocking events? *J. Atmos. Sci.*, **65**, 1442–1454.

Thompson, D. W. J., M. P. Baldwin, and J. M. Wallace, 2002: Stratospheric connection to northern hemisphere wintertime weather: Implications for prediction. *Journal of Climate*, **15 (12)**, 1421–1428.

Trenberth, K. E. and C. J. Guillemot, 1996: Physical processes involved in the 1988 drought and 1993 floods in north america. *J. Clim.*, **9 (6)**, 1288–1298.

Trenberth, K. E. and D. P. Stepaniak, 2002: A pathological problem with NCEP Reanalyses in the stratosphere. *Journal of Climate*, **15 (6)**, 690–695.

Woollings, T., A. Charlton-Perez, S. Ineson, A. G. Marshall, and G. Masato, 2010: Associations between stratospheric variability and tropospheric blocking. *Journal of Geophysical Research: Atmospheres*, **115 (D6)**.